

**Short title:** PHYs temperature perception and plastid metabolism

**PHYTOCHROME-DEPENDENT TEMPERATURE PERCEPTION MODULATES  
ISOPRENOID METABOLISM**

Ricardo Bianchetti<sup>1‡</sup>, Belen De Luca<sup>2‡</sup>, Luis A de Haro<sup>2†</sup>, Daniele Rosado<sup>1††</sup>, Diego Demarco<sup>1</sup>, Mariana Conte<sup>3</sup>, Luisa Bermudez<sup>3,4</sup>, Luciano Freschi<sup>1</sup>, Alisdair R. Fernie<sup>5</sup>, Louise V Michaelson<sup>6</sup>, Richard P Haslam<sup>6</sup>, Magdalena Rossi<sup>1‡</sup>, Fernando Carrari<sup>2,4‡\*</sup>

<sup>1</sup>Departamento de Botânica, Instituto de Biociências, Universidade de São Paulo, São Paulo, Brasil.

<sup>2</sup>Instituto de Fisiología, Biología Molecular y Neurociencias (IFIBYNE-UBA-CONICET) Ciudad Universitaria, C1428EHA Buenos Aires, Argentina.

<sup>3</sup>Instituto de Agrobiotecnología y Biología Molecular (IABIMO), CICVyA - INTA; CONICET, Argentina.

<sup>4</sup>Cátedra de Genética, Facultad de Agronomía, Universidad de Buenos Aires, Buenos Aires, Argentina.

<sup>5</sup>Max Planck Institute of Molecular Plant Physiology, Wissenschaftspark Golm, Am Mühlenberg 1, Potsdam-Golm, D-14476, Germany.

<sup>6</sup>Department of Plant Sciences, Rothamsted Research, Harpenden, Herts, AL5 2JQ, UK.

<sup>†</sup>Current address: Department of Plant and Environmental Sciences, Weizmann Institute of Science, Rehovot 76100, Israel

<sup>††</sup>Current address: Cold Spring Harbor Laboratory, 1 Bungtown Road, Cold Spring Harbor, New York 11724, USA

\* Corresponding Author.

Fernando Carrari

Phone: +54 11 4576-3386 / 3368 ext 238

email: [fcarrari@fbmc.fcen.uba.ar](mailto:fcarrari@fbmc.fcen.uba.ar)

‡ These authors contributed equally to this work.

**One-sentence summary:** Phytochrome-mediated temperature perception compromises plastidial development and function, impairing isoprenoid metabolism in tomato leaves and fruits.

## Author contributions

RB performed most of the experiments and analyzed the data; BDL and LAH performed experiments and analyzed data; DR, DD and LB performed experiments; MC, LF, ARF, LVM and RPH contributed to experimental design and provided technical assistance; RB, MR, ARF and FC conceived the project, designed experiments and wrote the paper which was revised and approved by all authors. FC agrees to serve as the author responsible for contact and ensures communication.

## FUNDING

This work was supported by FAPESP (Fundação de Amparo à Pesquisa do Estado de São Paulo, Grant Number #2016/01128-9); CNPq (Conselho Nacional de Desenvolvimento Científico e Tecnológico, Grant Number 440976/2016-2); European Union Horizon 2020 Research and Innovation Programme (Grant Agreement Number 679796), and ANPCyT Agencia Nacional de Promoción Científica y Tecnológica, Argentina, Grant Number 2014-0984 to F.C.). R.P.H and L.V.M. were supported by the BBSRC (Biotechnology and Biological Sciences Research Council, UK) through the Tailoring Plant Metabolism Institute Strategic Grant (BBS/E/C/000I0420) supporting R.P.H and the UK-Brazil Alliance for Sustainable Agriculture scheme (BBS/OS/NW/000001). R.B. and D.R. were recipient of FAPESP fellowships (#2017/24354-7 and #2015/14658-3). B.D.L and L.A.de H. are CONICET fellows. L.B. and F.C are members of CONICET. M.R. was a recipient of CNPq fellowship.

## Abstract

Changes in environmental temperature influence many aspects of plant metabolism; however, the underlying regulatory mechanisms remain poorly understood. In addition to their role in light perception, phytochromes (PHYs) have been recently recognized as temperature sensors affecting plant growth. In particular, in *Arabidopsis thaliana*, high temperature reversibly inactivates PHYB, reducing photomorphogenesis-dependent responses. Here, we show the role of phytochrome-dependent temperature perception in modulating the accumulation of isoprenoid-derived compounds in tomato (*Solanum lycopersicum*) leaves and fruits. The growth of tomato plants under contrasting temperature regimes revealed that high temperatures resulted in co-ordinated up-regulation of chlorophyll catabolic genes, impairment of chloroplast biogenesis, and reduction of carotenoid synthesis in leaves in a PHYB1B2-dependent manner. Furthermore, by assessing a triple *phyAB1B2* mutant and fruit-specific *PHYA*- or *PHYB2*-silenced plants, we demonstrated that biosynthesis of the major tomato fruit carotenoid, lycopene, is sensitive to fruit-localized PHY-dependent temperature perception. The collected data provide compelling evidence concerning the impact of PHY-mediated temperature perception on plastid metabolism in both leaves and fruit, specifically on the accumulation of isoprenoid-derived compounds.

**Keywords:** carotenoid, chlorophyll, chloroplast, fleshy fruit, isoprenoids, phytochrome, temperature, tomato.

## INTRODUCTION

Temperature cues regulate plant primary and secondary metabolism, affecting several agronomically important traits in crop species (Suwa et al., 2010; Bitá and Gerats, 2013; Zhao et al., 2017). It has been established that heat disrupts chloroplast integrity leading to further deficiencies of plastid-associated metabolites and a subsequent decline in plant performance (Yamori and von Caemmerer, 2009; Spicher et al., 2017). The ability to perceive stress conditions allows plants to adapt their metabolism in order to minimize any harmful effects on fitness (Saidi et al., 2011).

PHYTOCHROMES (PHYs) have been extensively described as light receptors. The biologically inactive PHY form (Pr) remains in the cytosol; however, once activated by red light, the active form (Pfr) is translocated towards the nucleus where it assembles into photobodies and triggers photomorphogenesis-associated responses (Rockwell et al., 2006). The conversion of Pr to Pfr can be reversed by far-red light or darkness (Burgie and Vierstra, 2014). PHYTOCHROME B (PHYB) has been associated with a quantitative trait loci interval for thermoresponsive growth in *Arabidopsis thaliana* (Box et al., 2015). High temperature reduces the abundance of Pfr by a quick and spontaneous reversion to Pr in a light-independent manner, consequently decreasing the size of nuclear bodies in a process termed thermoreversion (Legris et al., 2016). By contrast, lack of thermoreversion was detected in the hyperactive *phyB* mutant resulting in the constitutive presence of photobodies regardless of temperature condition (Huang et al., 2019). As such, the *A. thaliana phyB* null mutant mimics the transcriptional profile and physiological parameters of the wild-type counterpart grown under high temperature (Jung et al., 2016).

In tomato (*Solanum lycopersicum*) PHYs belong to a multigenic family encompassing five members: PHYA, PHYB1, PHYB2, PHYE, and PHYF (Alba et al., 2000b). We have previously demonstrated that PHYA, PHYB1, and PHYB2 positively control the biosynthesis of isoprenoid-derived compounds in tomato fruits in response to light (Bianchetti et al., 2018; Gramegna et al., 2018). PHYs post-translationally downregulate a group of helix-loop-helix proteins named PHYTOCHROME INTERACTING FACTORS (PIFs) (Park et al., 2018). PIFs derive from a multigenic family and have undergone sub- and neofunctionalization at the mRNA level (Rosado et al., 2016). It has been shown that SIPIF1a, SIPIF3, and SIPIF4 regulate carotenogenesis (Llorente et al., 2016), tocopherol

105 biosynthesis (Gramegna et al., 2018), and sugar metabolism (Rosado et al., 2019),  
106 respectively, by (a) light-dependant mechanism(s).

107 Here, by analyzing the metabolic and transcriptional profile of wild-type and *phy*-mutant  
108 tomato plants grown under contrasting temperature conditions, we showed that high  
109 temperature results in the reduction of leaf chlorophyll (Chl) and carotenoid levels in a  
110 PHYB1/B2-mediated manner through the regulation of Chl degradation and carotenoid  
111 biosynthetic genes, respectively. Furthermore, our data also demonstrate that high  
112 temperature or PHYAB1B2 impairment leads to the transcriptional downregulation of  
113 carotenoid biosynthetic genes in fruits, resulting in reduced levels of lycopene. Data  
114 obtained from fruit-specific *PHYA*- and *PHYB2*-silenced plants corroborated the role of  
115 fruit-localized PHYs in carotenoid accumulation through an intricate network in which  
116 master ripening transcription factors participate as mediators of temperature perception in  
117 tomato fruits.

## RESULTS

### High temperature affects plants growth phenotype in tomato

To investigate the role played by PHYs in response to high temperature, 20-day-old plants from wild type cv. MoneyMaker (MM), *phyB1* and *phyB2* single mutants, and the *phyB1B2* double mutant were transferred to ambient-temperature (AT, 24°C/18°C) and high-temperature (HT, 30°C/24°C) growing conditions (Supplemental Figure S1). Thirty days post-transfer, *phy* mutants displayed more elongated internodes than MM adult plants, as previously described (Kerckhoffs et al., 1997; 1997) under both temperature regimes, indicating that this is a genotype-dependent phenotype. On the other hand, for all the genotypes, HT promoted a narrower stem diameter, reduced leaf area, and less branching (Figure 1A), exposing a HT-dependent phenotype. Thus, in these plants, no PHY-dependent HT phenotype was observed, which contrasted with that described in *A. thaliana* seedlings, where HT increases elongation in a PHY-mediated manner (Jung et al., 2016). Moreover, no differences in relative water contents in leaves and fruits were observed between either genotypes or treatments (Supplemental Figure S2). These results indicate that the applied temperature treatments affected plant growth without changing the water status of the plants, rendering the experimental setup suitable to study the impact of temperature on tomato metabolism in a PHY-dependent manner.

### High temperature alters chlorophyll metabolism and fluorescence parameters in a PHYB1/B2-dependent manner

Evidences about the role of PHYB on Chl biosynthesis (Inagaki et al., 2015) and its function as a thermosensor in *A. thaliana* (Jung et al., 2016; Legris et al., 2017) led us to investigate the effects of PHYB1/B2-dependent temperature perception on tomato Chl metabolism. To address this question, Chl levels and fluorescence parameters were analyzed in leaves from 85-day-old plants of *phyB1*, *phyB2*, and *phyB1B2* mutants alongside the corresponding wild-type genotype. Notably, HT resulted in a significant reduction of total leaf Chl content in MM genotype. However, the mutants were virtually insensitive to this temperature effect. Interestingly, regardless of the temperature treatment, leaf Chl content in the *phyB1B2* double mutant was the same as that observed in MM under

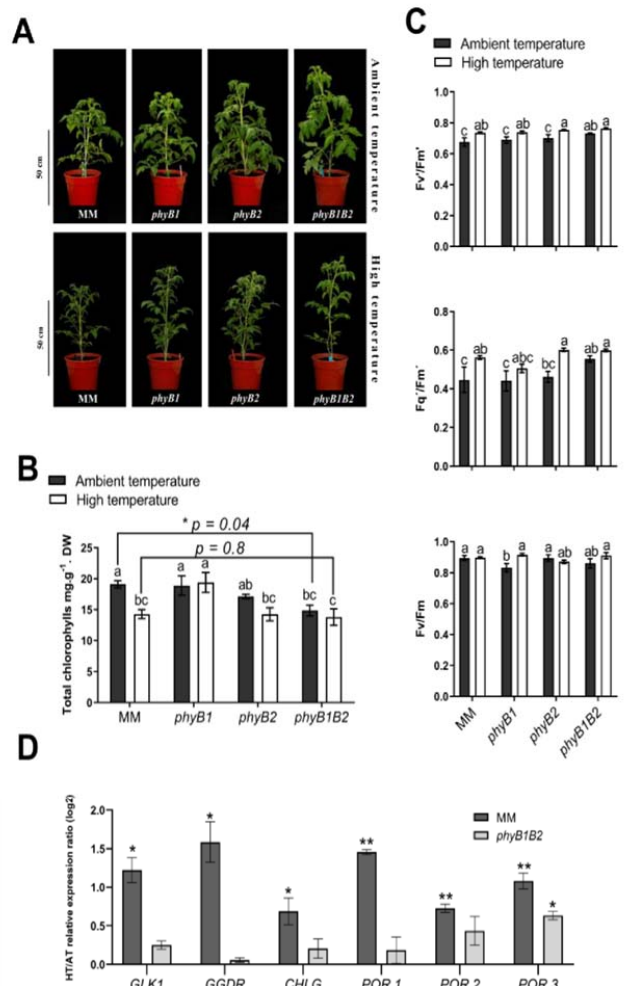


**Fig. 1. PHYB1/B2 are involved in temperature perception impacting leaf chlorophyll metabolism and fluorescence parameters in tomato.** (A) Side view of 50-day-old *S. lycopersicum* cv. Moneymaker (MM) plants and *phyB1*, *phyB2* and *phyB1B2* knockout mutants grown under ambient (AT, day/night 24 °C/18 °C) and high-temperature (HT, day/night 30 °C/24 °C). (B) Quantification of total chlorophylls in the seventh fully expanded leaf from 85-day-old plants. Each bar represents mean  $\pm$  SE (C) PSII maximum efficiency ( $F_v/F_m'$ ), PSII operating efficiency ( $F_q/F_m'$ ) and maximum quantum efficiency of PSII ( $F_v/F_m$ ) measured in the sixth fully expanded leaf from 85-days-old plants.  $n =$  at least five biological replicates. Each bar represents mean  $\pm$  SE. Different letters indicate statistically significant differences according to Fisher's multiple comparison test ( $p < 0.05$ ). Asterisks (\*)  $p < 0.05$ , \*\*  $p < 0.01$  indicate statistically significant differences by two-tailed Student *t* test between MM and *phyB1B2* in the same environmental condition. (D) HT/AT relative expression ratio of *GLK1*, *GGDR*, *CHLG*, *POR1*, *POR2* and *POR3* mRNA abundance in MM and *phyB1B2* mutant leaf samples from 85-days-old plants.  $n =$  at least three biological replicates. Each bar represents mean  $\pm$  SE. Asterisks (\*)  $p < 0.05$ , \*\*  $p < 0.01$  indicate statistically significant differences by two-tailed Student *t* test between AT and HT within the same genotype. Genes are denoted according to the abbreviations: *GLK1*, GOLDEN2-LIKE1; *GGDR*, GERANYLGERANYL DIPHOSPHATE REDUCTASE; *CHLG*, CHLOROPHYLL SYNTHASE; *POR*, PROTOCHLOROPHYLLIDE OXIDOREDUCTASE.

151 HT (Figure 1B). Additionally, under both temperature conditions, the *phyB1B2* double

mutant, but not the *phyB1* or *phyB2* single mutants, exhibited values of light-adapted PSII maximum efficiency ( $F_v'/F_m'$ ) and PSII operating levels ( $F_q'/F_m'$ ) similar to those observed in MM under HT conditions and higher than MM under AT conditions. No impact of HT on dark-adapted PSII maximum quantum efficiency ( $F_v/F_m$ ) was observed in any genotype (Figure 1C).

In order to gain insights into the regulatory role of PHYB1/B2 as temperature mediators in Chl metabolism, we further investigated the mRNA levels of genes encoding key proteins involved in Chl biosynthesis that previously showed PHY-dependent transcriptional regulation (Gramegna et al., 2018; Alves et al., 2020). These genes included *GERANYLGERANYL DIPHOSPHATE REDUCTASE* (*GGDR*), the last enzyme for phytyl diphosphate (PDP) chain synthesis (Almeida et al., 2015); the tetrapyrrole biosynthetic gene *PROTOCHLOROPHYLLIDE OXIDOREDUCTASE* (*POR*; three *loci* exist in the tomato genome named *POR1* (Solyc12g013710), *POR2* (Solyc10g006900) and *POR3* (Solyc07g054210), as revealed by the phylogenetic analyses presented in Supplemental Figure S3); and *CHLOROPHYLL SYNTHASE* (*CHLG*), which condensates the tetrapyrrole ring with the PDP (Almeida et al., 2015). Additionally, as a marker of chloroplast biogenesis and activity, we also included in the analysis the master transcriptional factor *GOLDEN2-LIKE1* (*GLK1*) (Nguyen et al., 2014), which regulates the expression of Chl biosynthetic genes (Nakamura et al., 2009). HT resulted in significant increases in *GLK1*, *GGDR*, *CHLG*, *POR1*, *POR2*, and *POR3* mRNA levels in the leaves of MM genotype, whereas *phyB1B2* double mutant displayed a constitutive HT phenotype regarding expression of Chl biosynthetic genes (except for the case of *POR3*, Figure 1D, Supplemental Table S1), exposing a PHYB1/B2-dependent induction of Chl biosynthesis under HT conditions.

Taken together, these results show that Chl accumulation is regulated by temperature in a PHYB1/B2-dependent manner synergistically, and reveal that temperature-induced Chl reduction is not the consequence of PHY-mediated impairment in Chl biosynthesis.

## **High temperature and PHYB1/B2 deficiency impact chloroplast biogenesis and differentiation**



The effect of PHYs (Oh and Montgomery, 2014; Martin et al., 2016) and temperature (Takahashi and Murata, 2008; Van Eerden, et al., 2015) on chloroplast biogenesis and structure have already been studied separately in several plant species. However, these two variables have not been previously assayed in an integrated manner in tomato, nor have they been assessed in any other crop species where chloroplasts determine nutritional quality. Here, we evaluated whether the HT-induced impact on chloroplast development is mediated by PHYB1/B2 in tomato. Similarly to that observed for 85-day-old plants (Figure 1B), 21-day-old plants of MM, grown under HT conditions, and the *phyB1B2* mutant, regardless of the temperature condition, showed chlorotic symptoms (red arrows Figure 2A). This visual phenotypic difference agreed with lower measurements of leaf Chl content (Figure 2B), strengthening the idea of PHYB1/B2 as a mediator of temperature perception modulating leaf Chl metabolism. Thus, to address whether differences in Chl levels were associated with changes in chloroplast biology, plastid quantification and ultrastructure analyses were performed in mesophyll cells. Microscopy data revealed a reduction in the number of chloroplasts per mesophyll cell in MM plants grown under HT and in the *phyB1B2* double mutant cells under AT and HT compared to MM genotype under AT (Figure 2C). Interestingly, the *phyB1B2* double mutant still showed a slight temperature response, indicating the existence of PHY-independent temperature sensing, as reported in *A. thaliana* (Fujii et al., 2017; Ma et al., 2016). Additionally, leaves developed under HT exhibited remarkable changes in chloroplasts ultrastructure (Figure 2D). Chloroplasts of MM developed under HT and those of the *phyB1B2* double mutant, under both temperature regimes, showed reduced grana stacking and dilated thylakoid lumen in comparison to MM under AT.

PIF transcription factors have shown to mediate PHY-dependent temperature perception and, in particular PIF1 and PIF3, have been shown to regulate chloroplast development in *A. thaliana* (Kim et al., 2016, Stephenson et al., 2009). In tomato PIF4 has been shown to participate in temperature-dependent seedling elongation (Rosado et al., 2019). Although PIFs accumulation is mostly regulated post-translationally, we found that *PIF1b* mRNA levels increase under HT in the MM genotype but the *phyB1B2* double mutant was insensitive (Supplemental Figure S4A). We also identified significant upregulation of *PIF3* mRNA in response to HT in MM and in the *phyB1B2* mutant regardless of temperature.

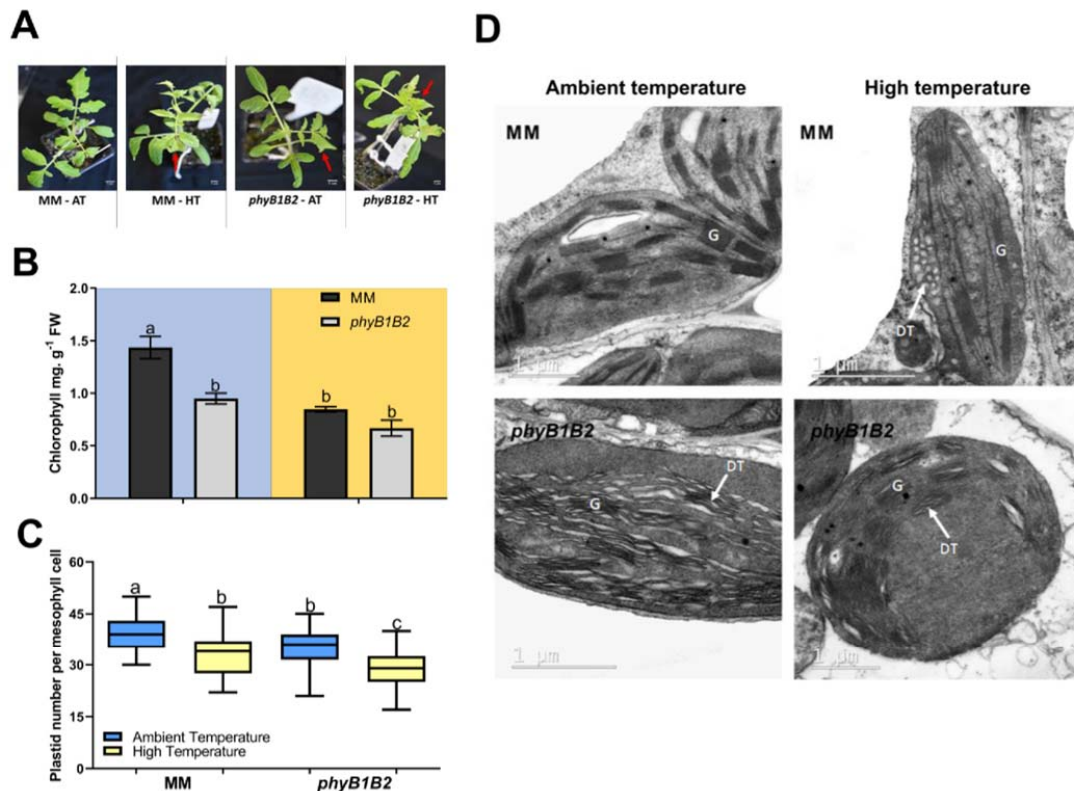


**Figure 2. High temperature affects plastid biogenesis and development in leaves in a PHYB1/B2-dependent manner.** (A) Visualization of a representative leaf of 21-day-old *S. lycopersicum* cv. Moneymaker (MM) and *phyB1B2* knockout mutants after two weeks under ambient (AT, day/night 24 °C/18 °C) and high-temperature (HT, 30 °C/24 °C). Red arrows indicate chlorotic leaves (MM at HT, *phyB1B2* at AT and *phyB1B2* at HT). (B) Quantification of total chlorophylls in leaves cultivated under AT (blue background) and HT (yellow background). n = at least three biologically replicates. Each bar represents mean ± SE. (C) Plastid density per mesophyll cell. Values represent chloroplast quantification of ± 70 cells. Different letters indicate statistically significant differences according to Fisher's multiple comparison test ( $p < 0.05$ ). Each bar represents mean ± SE. (D) Representative TEM images of chloroplast from MM and *phyB1B2* leaves grown under AT and HT. G indicates grana and DT indicated dilated thylakoids.

These alterations in *PIF1b* and *PIF3* mRNA levels may explain, at least in part, the reduced number of plastids and their altered ultrastructure.

In conclusion, our data suggest that temperature perception mediated by PHYB1/2 has an impact on chloroplast development that ultimately determines their structure and function.

**PHYB1/B2 inactivation mediated by high temperature enhances chlorophyll degradation pathway in leaves**

In *A. thaliana*, PHYB regulates leaf senescence in response to light conditions through PIF4/PIF5, which in turn induce Chl breakdown (Sakuraba et al., 2014). However, it is unknown how PHYB-mediated temperature perception operates on Chl catabolism. The Chl degradation pathway operates in tomato leaves during senescence (Lira et al., 2014; Guyer et al., 2014), leading to phytol chain removal followed by the linearization of the tetrapyrrole ring involving several enzymatic steps (Hörtensteiner, 2013; summarized in Figure 3A). In brief, Chl *a* is converted to an intermediate phytol-free chlorophyllide *a* (Chlide *a*) or a magnesium-free pheophytin *a* (Pheo *a*) form by CHLOROPHYLLASE (CLH) and STAY GREEN (SGR), respectively. Chlide *a* and Pheo *a* are subsequently converted into pheophorbide *a* (Pheide *a*) through dechelation, mediated by STAY GREEN-LIKE (SGR-like), and dephytylation, mediated by PHEOPHYTINASE (PPH), respectively. Finally, Pheide *a* is linearized by PHEOPHORBIDE A OXYGENASE (PAO) to yield a red chlorophyll catabolite (RCC). To understand Chl reductions observed under HT and in the *phyB1B2* mutant, we therefore measured the mRNA levels of *CLH1*, *CLH2*, *CLH4*, *SGR*, *PPH*, *SGR-like*, and *PAO*.

mRNA levels of *CLH2*, *CLH4*, *PPH*, *SGR-like*, and *PAO* were at least two-fold up-regulated in MM plants cultivated under HT (Figure 3B). Consistent with our proposed role of PHYB1/B2 in temperature perception, regardless of the temperature condition, the *phyB1B2* double mutant showed mRNA levels similar to those observed in MM under HT for the *CLH4*, *PPH*, *SGR-like*, and *PAO* genes (Figure 3A and Figure 3B). It has been reported that Chl degradation is triggered by dark-induced senescence and mediated by PHY perception and PIF signaling (Sakuraba et al., 2014). In particular, SGR and PAO enzyme-encoding genes are directly upregulated by PIF4 and PIF5 in *A. thaliana* (Song et al., 2014; Zhang et al., 2015). Even though the *PIF4* mRNA profile did not respond to temperature in our experiment (Supplemental Figure S4A), we cannot formally rule out its involvement in the regulation of this process, considering that we were able to identify PIF-binding motifs in the four genes that showed PHYB1/B2-mediated temperature modulation, specifically *CLH4*, *PPH*, *SGR-like*, and *PAO* (Supplemental Figure S4B). This observation suggests that the PHY-PIF module acts similarly in tomato as in *A. thaliana*.

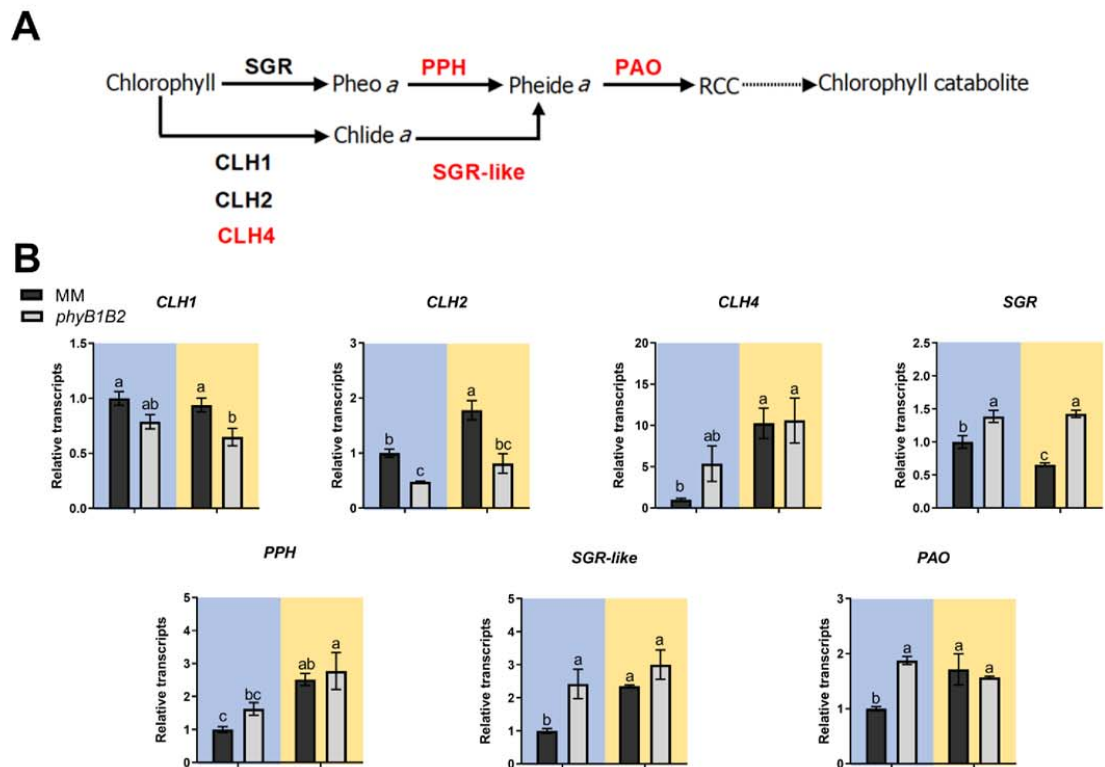


**Figure 3. High temperature enhances chlorophyll degradation in leaves in a PHYB1/B2-dependent manner.**

(A) Schematic model of chlorophyll degradation pathway. Enzymes and metabolites are denoted according to the following abbreviations: Pheo *a*, pheophytin *a*; Chlide *a*, chlorophyllide *a*; Pheide *a*, pheophorbide *a*; RCC, red chlorophyll catabolite; CLH, CHLOROPHYLLASE; SGR, STAY GREEN; SGR-like, PPH, PHEOPHYTINASE; STAY GREEN-LIKE; PAO, PHEOPHORBIDE *a* OXYGENASE. The enzymes highlighted in red are those that showed to be regulated by temperature in a PHYB1/B2-dependent manner according to Figure 3B. (B) Relative mRNA levels of chlorophyll degrading enzymes encoding genes in Moneymaker (MM) and *phyB1B2* mutant leaf samples from 85-day-old plants grown under ambient temperature (AT, 24 °C/18 °C - blue background) and high-temperature (HT, 30 °C/24 °C - yellow background). Expression levels are relative to MM – AT condition. n = at least three biological replicates. Each bar represents mean ± SE. Different letters indicate statistically significant differences according to Fisher's multiple comparison test ( $p < 0.05$ ).

Collectively, these results demonstrated that PHYB1/B2 represses Chl catabolism genes in a temperature-dependent manner in tomato leaves.

**PHYB1/B2-dependent temperature perception regulates leaf carotenoid biosynthesis at the transcriptional level**

Alongside the induction of the Chl degradation pathway, the HT treatment and the *phyB1B2* double mutation resulted in over 30% reduction of total leaf carotenoids (Figure 4A). To understand the molecular basis of this reduction, we analyzed the transcriptional profile of carotenoid biosynthetic enzyme-encoding genes. *GERANYLGERANYL DIPHOSPHATE SYNTHASE 1* (*GGPS1*), which produces the carotenoids precursor geranylgeranyl diphosphate (Quadrana et al., 2013), was shown to be downregulated both in response to HT and in the *phyB1B2* double mutant (Figure 4B). By contrast, genes encoding carotenoid downstream enzymes, such as PHYTOENE SYNTHASE 2 (*PSY2*), PHYTOENE DESATURASE (*PDS*), CHROMOPLAST-SPECIFIC LYCOPENE  $\beta$  CYCLASE (*CYC $\beta$* ), and CHLOROPLAST-SPECIFIC LYCOPENE  $\beta$  CYCLASE (*LYC $\beta$* ), did not show PHYB1/B2-mediated temperature modulation (Supplemental Figure S5). Thus, the results presented above indicate that, in tomato leaves, the accumulation of chloroplast photosynthetic pigments is controlled through transcriptional adjustments of Chl degradation and carotenoid biosynthesis genes by the ambient temperature in a PHYB1/B2-dependent manner.

## **Fruit carotenoid contents are modulated by temperature through PHYA and PHYB1/B2**

A role for PHYs in tomato fruit carotenoid accumulation has long been proposed (Alba et al., 2000a; Gupta et al., 2014), and we recently demonstrated that fruit-localized PHYA and PHYB2 positively influence fruit carotenoid accumulation (Bianchetti et al., 2018). Aiming to evaluate the temperature effects on carotenogenesis, we followed two complementary approaches: i) investigate the single *phyA*, *phyB1*, and *phyB2* mutants and the triple *phyAB1B2* mutant and ii) analyze fruit-specific RNAi *PHYA*- and *PHYB*-silenced lines in the Micro-Tom (MT) background (*PHYA*<sup>RNAi</sup> and *PHYB2*<sup>RNAi</sup>). This would allow us to unravel whether fruit-localized PHYs regulate carotenogenesis in a temperature-dependent manner in this organ and if this mechanism is genotype-independent.

Except for the *phyAB1B2* triple mutant, ripe fruits harvested from HT-grown plants exhibited reductions in total carotenoid content compared to that in AT counterparts (Figure 5A). Ripe fruits collected from single *phyA*-, *phyB1*-, and *phyB*-mutant plants or double *phyB1B2*-mutant plants grown under AT displayed lower total carotenoid levels those that

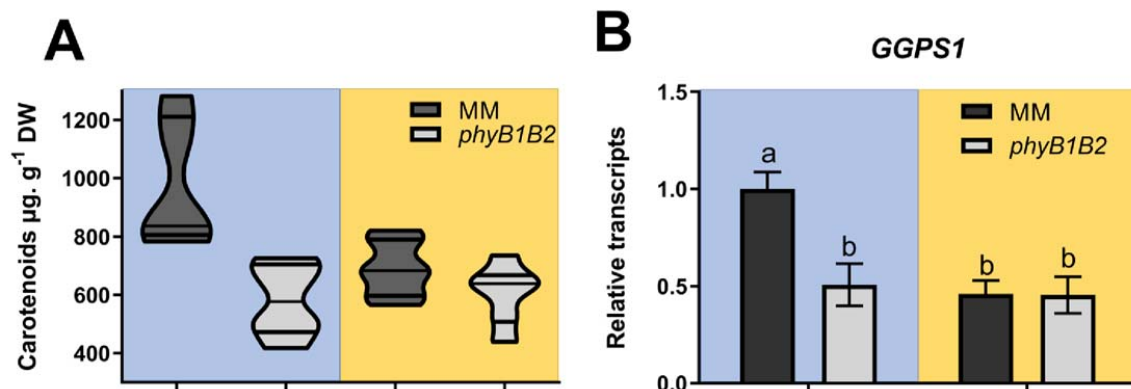


**Figure 4. PHYB1/B2-dependent temperature perception transcriptionally regulates leaf carotenogenesis.**

(A) Total carotenoid levels expressed in µg per g of dry weight. *n* = at least five biological replicates. (B) Relative mRNA levels of *GGPS1* gene in Moneymaker (MM) and *phyB1B2* mutant leaf samples from 85-day-old plants grown under ambient temperature (AT, 24 °C/18 °C - blue background) and high-temperature (HT, 30 °C/24 °C - yellow background). Expression levels are relative to MM – AT condition. *n* = at least three biological replicates. Each bar represents mean ± SE. Different letters indicate statistically significant differences according to Fisher's multiple comparison test (*p* < 0.05). Gene is denoted according to the abbreviation: *GGPS1*, GERANYLGERANYL PHOSPHATE SYNTHASE 1.

in MM counterparts. Interestingly, an enhanced reduction was observed in the *phyAB1B2* triple mutant, which displayed similar total fruit carotenoid levels under both temperature regimes (Figure 5A). High-performance liquid chromatography (HPLC) carotenoid profiling revealed that accumulation of lycopene, alongside its precursors phytoene and phytofluene, was reduced by HT compared to AT in all genotypes aside from in the triple *phyAB1B2* mutant, which showed similar profiles of phytoene, phytofluene, and lycopene in fruits developed under both temperature regimes (Supplemental Figure S6 and Figure 5B).

To investigate whether the temperature-mediated reduction in carotenoid content is a consequence of the transcriptional regulation of carotenoid biosynthetic genes, we further profiled *GGPS2*, *PSY1*, and *PDS* mRNA abundances in MM and the *phyAB1B2* triple mutant. In agreement with enhanced carotenoid biosynthesis during ripening, the three analyzed genes displayed a clear induction in MM under AT at the onset of ripening (from mature green to breaker stages). At the mature green stage, no significant difference in expression was observed attributable to genotype or temperature treatment. However, at



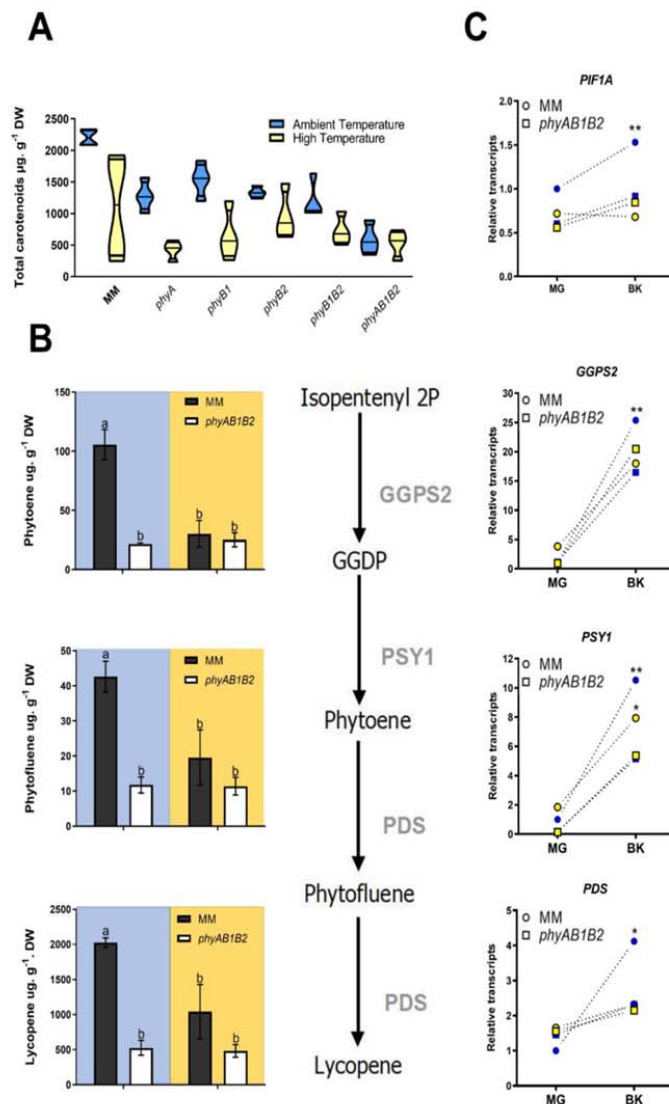


**Figure 5. PHYA/B1/B2-dependent temperature perception transcriptionally regulates fruit carotenogenesis.** (A) Total carotenoid (phytoene, phytofluene, lycopene, lutein and  $\beta$ -carotene) levels quantified from ripe fruits of Moneymaker (MM) and *phyA*, *phyB1*, *phyB2*, *phyB1B2* and *phyAB1B2* mutant plants grown under ambient (AT, blue, day/night 24 °C/18 °C) and high-temperature (HT, yellow, day/night 30 °C/24 °C). (B) Center: schematic model of lycopene biosynthetic pathway, the dotted line represents more than one enzymatic step. Left: levels of lycopene, phytoene and phytofluene in ripe fruits. AT: blue background; HT: yellow background. Each bar represents mean  $\pm$  SE. Different letters indicate statistically significant differences according to Fisher's multiple comparison test ( $p < 0.05$ ). Right: Relative mRNA levels from carotenoids biosynthetic genes *GGPS2*, *PSY1* and *PDS* in fruits at mature green (MG) and breaker (BK) stages harvested from plants grown at AT (blue) and HT (yellow). Transcripts levels are expressed relative to MM MG – AT condition. Asterisks (\*  $p < 0.05$ , \*\*  $p < 0.01$ ) indicate differences in the analysis of variance in a multiple comparison test within the same fruit stage. Metabolites and genes are denoted according to the following abbreviations: GGDP, geranylgeranyl diphosphate; *GGPS2*, GERANYLGERANYL PHOSPHATE SYNTHASE 2; *PSY1*, PHYTOENE SYNTHASE 1; *PDS*, PHYTOENE DESATURASE. (C) Relative mRNA levels of *PIF1a* carotenogenesis regulator gene in fruits at mature green (MG) and breaker (BK) stages harvested from plants grown at AT (blue) and HT (yellow). Transcripts levels are expressed relative to MM MG – AT condition. Asterisks (\*\*  $p < 0.01$ ) indicate differences in the analysis of variance in a multiple comparison test within the same fruit stage.

300 breaker stage, *GGPS2*, *PSY1*, and *PDS* mRNA levels were downregulated in response to 12

both temperature and the triple *phyAB1B2* mutation (Figure 5B). The role of PIF1a in tomato fruit carotenogenesis has been previously reported. Although, upon induction of ripening, *PIF1a* transcript levels increased; concomitantly, Chl degradation alters the quality of the light filtered through the fruit pericarp, increasing the relative red/far-red ratio. As a consequence, PIF degradation increases, enhancing *PSY1* expression and carotenoid accumulation (Llorente et al., 2016). Indeed, our results revealed PIF1a upregulation from MG to BK stage in MM grown under AT, but its levels remained invariable in both genotypes under HT (Figure 5C).

In summary, the temperature-insensitive phenotype observed in the *phyAB1B2* triple-mutant fruits revealed that the inductive effect of PHYA/B1/B2 over the transcription of carotenogenesis-associated genes is abolished by HT conditions.

In order to mitigate the influence of any possible pleiotropic effect of *phy* mutations at the whole-plant level, we further analyzed fruit carotenoid accumulation in fruit-specific *PHYA*- and *PHYB2*-silenced lines, namely *PHYA*<sup>RNAi</sup> and *PHYB2*<sup>RNAi</sup>. Regardless of temperature, the lycopene content in *PHYA*<sup>RNAi</sup> or *PHYB2*<sup>RNAi</sup> fruit was reduced by half in comparison to control fruits developed under AT, the latter of which were affected by HT conditions (Figure 6A). It is worth noting that this effect was observed in two independent transgenic lines for each genotype (Supplemental Figure S7). In agreement, *PSY1* transcript accumulation accompanied the variations observed in lycopene content (Figure 6B), confirming that fruit-localized PHY-mediated temperature perception controls carotenoids accumulation through transcriptional regulation of the biosynthetic enzyme-encoding genes.

### ***PHYA*- and *PHYB2*-mediated temperature perception controls carotenoids biosynthesis through master ripening transcription factors**

Besides *PIF1a* (Llorente et al., 2016), *PSY1* expression has been demonstrated to be regulated by ripening-associated transcription factors in tomato (Liu et al., 2015). For this reason, we profiled the mRNA levels of candidate genes encoding master ripening regulators, namely *APETALA2a* (*AP2a*), *NON-RIPENING* (*NOR*), *RIPENING INHIBITOR* (*RIN*), *TOMATO AGAMOUS-LIKE* (*TAGL1*), and *FRUITFULL1* and 2 (*FUL1/2*) (Klee and Giovannoni, 2011), in *PHY*<sup>RNAi</sup> lines subjected to both temperature regimes.



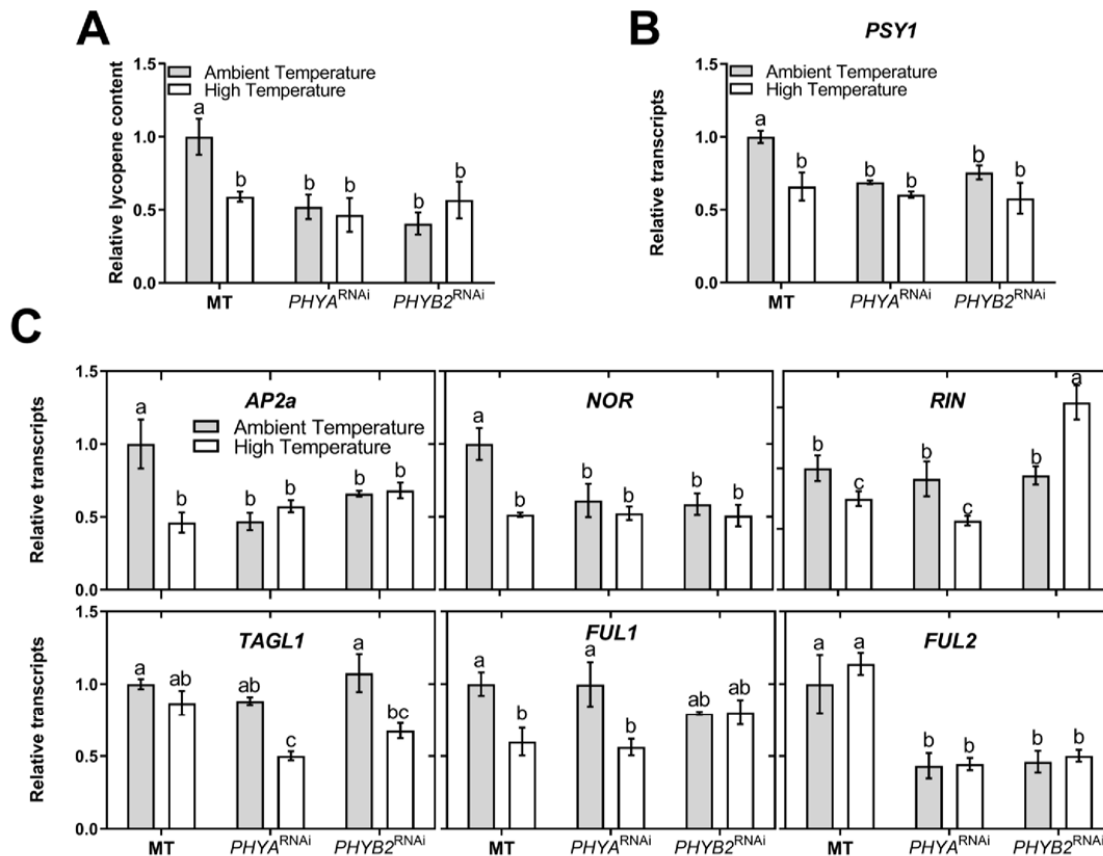


**Figure 6. Fruit-localized *PHYA* and *PHYB2* are involved in temperature perception impacting lycopene synthesis and master fruit ripening regulators.** (A) Lycopene levels quantified in ripe fruits from Micro-Tom (MT) control genotype and fruit-specific *PHYA*- (*PHYA*<sup>RNAi</sup>) and *PHYB2*- (*PHYB2*<sup>RNAi</sup>) knockdown transgenic lines grown under ambient (24 °C/18 °C) and high temperature (30 °C/24 °C). Lycopene levels were quantified and expressed relative to MT fruits at ambient temperature and values are means of at least three biological replicates from two independent lines for each genotype. Each bar represents mean ± SE. (B,C) Relative mRNA levels of (B) *PSY1* (C) and master fruit ripening regulator genes in MT, *PHYA*<sup>RNAi</sup> and *PHYB2*<sup>RNAi</sup> breaker fruit samples harvested under AT and HT. Expression levels are relative to MT – AT condition. n = at least three biological replicates. Each bar represents mean ± SE. Different letters indicate statistically significant differences according to Fisher's multiple comparison test ( $p < 0.05$ ). *RIN*; *RIPENING INHIBITOR*, *NOR*; *NON-RIPENING*, *FUL1*; *FRUITFULL1*, *FUL2*; *FRUITFULL2*, *AP2a*; *APETALA2a*, *TAGL1*; *TOMATO AGAMOUS-LIKE1*, *PSY1*; *PHYTOENE SYNTHASE 1*.

Three expression patterns were observed; i) *RIN*, *TAGL1*, and *FUL1* mRNA levels responded to temperature treatment and in certain cases these responses varied in the absence of *PHYA* or *PHYB2*, ii) *FUL2* was downregulated only in the lack of functional PHYs (*PHYA*<sup>RNAi</sup> or *PHYB2*<sup>RNAi</sup> lines), and iii) *AP2a* and *NOR* mRNAs displayed a clear

response to PHY-mediated temperature perception (Figure 6C). These results suggest that fruit-localized PHY-mediated temperature perception controls carotenoid accumulation via transcriptional regulation of ripening master controller genes.

Combined, these results decrypt the role of fruit-localized PHYA and PHYB1/B2 as temperature sensors in tomato fruits, which regulate carotenoid accumulation through the transcriptional control of genes involved in their biosynthesis by alternative and converging molecular pathways.

## DISCUSSION

Studies performed on plants under warm treatment or employing PHY-signalling defective mutants have demonstrated the synergistic influence of light and temperature on the regulation of chloroplast metabolism (Stephenson et al., 2009; Zhao et al., 2016; Spicher et al., 2016; Dubreuil, et al., 2017; Spicher et al., 2017). Despite this fact, the two factors have been studied independently, limiting our comprehensive understanding of light- and temperature-perception mechanisms at the molecular level. Recently, the role of PHYs as thermosensors by the gradual inactivation of PHYB by increasing temperature was reported in *A. thaliana* (Legris et al., 2017). However, whether this mechanism operates in crop species evolved in different environments, and how this PHY-dependent temperature signaling cascade impacts major metabolic pathways, remains poorly understood. It is worth mentioning that PHY-independent temperature responses have also been described associated with other photoreceptors (Fujii et al., 2017; Ma et al., 2016) and also in photoreceptor-impaired conditions (Legris et al., 2016). In accordance, we also observed PHY-independent temperature responses here (Figure 2C). In the current study, we present experimental evidence that central enzyme-encoding genes of Chl and carotenoid metabolism are regulated at the transcriptional level by PHYB1/B2- and PHYA/B1/B2-mediated temperature perception in tomato leaf chloroplasts and fruit chromoplasts, respectively.

Constitutive HT-induced features were previously observed in the *A. thaliana phyB* loss-of-function mutant (Jung et al., 2016; Huang et al., 2019). In contrast to the single-copy gene *PHYB* found in *A. thaliana* (Sharrock and Quail, 1989), the tomato genome harbors two *PHYB* paralogs, *PHYB1* and *PHYB2*, which originated during a genome triplication event in the Solanaceae common ancestor (Tomato Genome Consortium, 2012). Indeed, results from our current work indicate that loss-of-function in the double *phyB1B2* mutant, rather than single *phyB1* or *phyB2* mutations, is necessary to generate a thermoinsensitive phenotype in tomato leaves leading to a reduction in Chl content, indicating that PHYB1 and PHYB2 play additive functions as temperature sensors (Figure 1B). The *phyB1B2* double mutant did not show changes in the mRNA abundances of Chl biosynthetic genes in response to HT (Figure 1D). However, these genes were upregulated by HT in MM leaves,

which does not explain the low-Chl phenotype shown by these plants (Figure 1B) and suggests a highly complex regulatory mechanism.

Interestingly, together with the reduction in Chl content, increased Chl fluorescence parameters were registered (Figure 1C). Our results are consistent with the finding in *A. thaliana* that faster electron transport occurred under HT conditions acting as an electron sink for the increment in photorespiration (Zhang and Sharkey, 2009).

The observable decrease in total Chl has been associated with a decrease in the LHCII, serving as a protective mechanism in plants undergoing abiotic stress (Ishida et al., 2000). In agreement, we observed a reduction in chloroplast number and alterations in grana stacking (Figure 2), probably mediated by higher *PIF3* mRNA level in response to PHYB1B2-mediated temperature inactivation (Supplemental Figure S4A). In line with this, *PIF3* protein accumulation led to impaired chloroplast development in *A. thaliana* (Stephenson et al., 2009). Moreover, our results provide genetic evidence that HT and the *phyB1B2* mutation trigger Chl catabolism via the upregulation of genes associated with Chl degradation, i.e., *CLH4*, *PPH*, *SGR-like*, and *PAO* (Figure 3). It was recently demonstrated that *PIF4* regulates senescence in tomato (Rosado et al., 2019). Additionally, PHYs trigger *PIF4* degradation (Lorrain et al., 2008), avoiding its inductive role on Chl breakdown (Sakuraba et al., 2014; Song et al., 2014; Zhang et al., 2015). In this sense, several canonical PIF binding motifs, i.e., G- and PBE-box (Martínez-García et al., 2000; Zhang et al., 2013), were found in the promoter of the Chl degrading-associated genes mentioned above (Supplemental Figure S4B). Further reports extensively associate the inhibition of *PIF4* degradation in response to HT impacting several events throughout the plant cycle (Koini et al., 2009; Qiu et al., 2019; Zhou et al., 2019). Together, these data suggest that inactivation of PHYB1/B2 under HT affects Chl accumulation through altered chloroplast biogenesis (Figure 2) and degradation (Figure 3), likely via *PIF1b/PIF3*- and *PIF4*-dependent mechanism(s), respectively.

Our findings additionally indicate a down-regulation of *GGPSI* mRNA levels by temperature and the *phyB1B2* mutation (Figure 4B). Since GGPS is the last shared step between the Chl and carotenoid biosynthetic pathways (Cordoba et al., 2009), this result is in accordance with the impairment of Chl and carotenoid synthesis in the leaves under these conditions (Figure 2B,4A).

Besides the impact on vegetative organs, our data also indicated that HT negatively influences carotenoid accumulation in tomato fruits (Figure 5A). Alterations of isoprenoid-derived compounds in response to thermal stress have been increasingly demonstrated over the last years (Velikova et al., 2011; Spicher et al., 2016). Exposure of single, double, and triple PHY mutants as well as the MM control plants to two independent temperature regimes revealed a combinatory effect of temperature and the action of PHYs on carotenoid content of ripe fruits (Figure 5A). In contrast to the other genotypes analyzed, the reduced levels of fruit lycopene and their precursors observed in *phyAB1B2* might be due to impaired temperature perception in this genotype (Figure 5B). Consistent with this view, our findings indicate that the *phyAB1B2* mutations, as well as HT conditions, downregulate the expression of the major carotenoid biosynthetic genes, e.g., *GGPS2*, *PSYI*, and *PDS* (Figure 5B). This is in agreement with our previous report showing that these genes are transcriptionally regulated by PHY-mediated light perception in tomato fruit (Bianchetti et al., 2018).

To further examine whether the observed impact on fruit carotenoids was the effect of whole-plant PHY deficiency or those localized in the fruits, we analyzed fruit-specific RNAi *PHYA*- and *PHYB*-silenced lines in MT genetic background (Bianchetti et al., 2018). Results showed equivalent reductions of lycopene accumulation and *PSYI* transcript levels in both transgenic lines, showing temperature insensitivity (Figure 6A, 6B), demonstrating that fruit-localized PHYs act as thermosensors and that this effect is genotype independent. Indeed, the central role played by temperature and PHYs controlling *PSYI* expression (Figure 6B) is supported by previous studies demonstrating that PIF1a downregulates carotenoid biosynthesis via *PSYI* transcriptional repression in tomato fruits (Llorente et al., 2016), similarly as its ortholog in *A. thaliana* in response to temperature (Toledo-Ortiz et al., 2014). In addition to PIF1a, carotenoid biosynthesis in tomato fruit is markedly regulated at the transcriptional level by the master ripening transcription factors RIN, NOR, FUL1, FUL2, TAGL1, and AP2a (Klee and Giovannoni, 2011). Whereas a non-combined effect of fruit-specific *PHY* expression and temperature on *RIN*, *TAGL1*, *FUL1*, or *FUL2* transcript abundance was observed, *AP2a* and *NOR* mRNA levels responded to temperature in a PHY-dependent manner (Figure 6C), thus contributing to a reduction in lycopene content (Figure 6A), most likely by the transcriptional regulation of *PSYI*, as previously

described (Chung et al., 2010; Karlova et al., 2011; Yuan et al., 2016; Cruz et al., 2018). These results exposed an interesting network that regulates ripening in response to light and temperature in an independent or integrated way, warranting this key evolutionarily selected process.

Overall, our results support a model (Figure 7) where increases in temperature induce the inactivation of PHYs, probably through the conformational change from the biologically active Pfr to the inactive Pr form. The thermosensing role of PHYB1/B2 impacts leaf Chl and carotenoid levels through combined control of chloroplast biogenesis and the transcript levels of carotenoid biosynthetic and Chl degrading enzyme genes. Moreover, our data demonstrate that PHYA/PHYB1/PHYB2-mediated temperature perception modulates carotenoid metabolism in fruit. The data also showed the involvement of master ripening regulator genes as mediators of PHY-dependent temperature regulation of the carotenoid biosynthetic pathway. In conclusion, this study demonstrates the effect of PHY-mediated temperature perception on both photosynthetic and heterotrophic tomato plastid metabolism. Moreover, the results presented here identify the PHYs as critical hubs that can be manipulated to maintain and/or improve the nutritional quality of edible fruits in the context of global increasing temperatures.

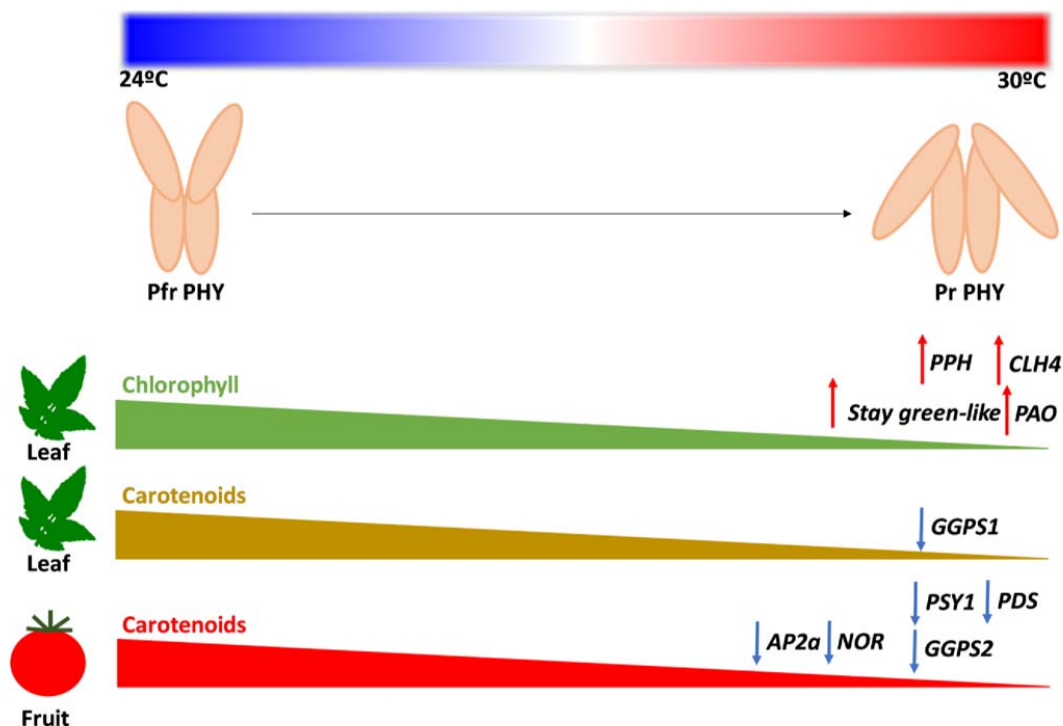


**Figure 7. The effect of PHY-mediated temperature perception on tomato metabolism regulation.** The rise of ambient temperature shifts balance to the inactive phytochrome (Pr) form, which promotes chlorophyll degradation pathway in source leaves through the transcriptional up-regulation of chlorophyll catabolic enzyme-associated genes. Additionally, reduced levels of Pfr impair carotenoid accumulation in both leaves and ripe fruits, through the transcriptional downregulation of carotenoid biosynthetic and master ripening regulator genes.

## METHODS

### Plant material, growth conditions, and sampling

*Solanum lycopersicum* plants (cv. MoneyMaker) harboring loss-of-function mutations in *phyA*, *phyB1*, *phyB2*, *phyB1B2*, and *phyAB1B2* were previously characterized (Kerckhoffs et al., 1996; Kerckhoffs et al., 1997; Lazarova et al., 1998a; Lazarova et al., 1998b; Kerckhoffs et al., 1999; Weller et al., 2000). Micro-Tom fruit-specific *PHYA*- and *PHYB2*-silenced lines (*PHYA*<sup>RNAi</sup> and *PHYB2*<sup>RNAi</sup>) were previously obtained and characterized by Bianchetti et al. (2018). Although the Micro-Tom cultivar is deficient in brassinosteroid biosynthesis due to the weak mutation *d*, it has been extensively demonstrated that it represents a convenient and adequate model system to study fruit biology (Campos et al.,

2010). In this work, we used Micro-Tom PHYA<sup>RNAi</sup> and PHYB2<sup>RNAi</sup> lines as a proof of concept that fruit-localized PHYs regulate carotenogenesis in a temperature-dependent manner in this organ and that this mechanism is genotype independent.

Tomato seeds (cv. MoneyMaker and Micro-Tom) were sown under standard greenhouse conditions (day/night 24°C/18°C, 16/8 h light/dark, and 60% air relative humidity) in Floricultura Z substrate. Twenty-day-old plants were transplanted to 9-L pots and cultivated for 120 days (16/8 h light/dark and 60% air relative humidity) in greenhouses under two distinct temperature regimens: ambient (24°C/18°C) and high (30°C/24°C) temperature with a mean daily difference of 5°C (Supplemental Figure S1A, B). These temperatures have been previously described as optimal and suboptimal high for tomato (Ayenan et al., 2019). Plants were cultivated under 250  $\mu\text{mol m}^{-2} \text{s}^{-1}$  light intensity, which is lower than the tomato saturation point (approximately 800  $\mu\text{mol m}^{-2} \text{s}^{-1}$ ). To avoid unwanted effects on plant water status (Fahad et al., 2017), the plants were watered twice a day and the relative ambient humidity was monitored (Supplemental Figure S1C). Leaves (seventh fully expanded leaf from bottom to top) and fruits [at mature green, breaker, and ripe (7 days after breaker) stages] from MoneyMaker background plants were harvested 65 and 80–110 days after the beginning of the temperature treatment. Fruits from Micro-Tom plants were harvested 75–90 days after the start of temperature treatment. Samples were ground in liquid N<sub>2</sub> and freeze-dried prior to subsequent analysis.

### Pigment quantification

Chlorophyll (Chl) extraction was carried out from 5 mg of freeze-dried leaf tissue in 1 mL of 80:20 acetone:Tris-HCl 100 mM pH 7.5. Samples were sonicated for 5 min at 42 kHz and further centrifuged at 16000  $\times g$  for 2 min. The supernatant was collected and the procedure was repeated until the green color was totally removed from the tissue. Spectrophotometer measurements were performed at 537, 647, 663, and 750 nm. Total Chl content was estimated by the equation:  $0.01373 \times (A_{663} - A_{750}) - 0.000897 \times (A_{537} - A_{750}) - 0.003046 \times (A_{647} - A_{750})$  (Sims and Gamon, 2003). For leaf carotenoid extraction, 5 mg of freeze-dried samples were immersed in 1 ml of *N,N*-dimethylformamide, sonicated for 5 min at 42 kHz, and centrifuged at 16000  $\times g$  for 5 min. Supernatant absorbance was recorded at 480, 647, and 664 nm, then carotenoid contents



were determined by the equation:  $\{1000 \times A_{480} - [1.12 \times (12 \times A_{664}) - (3.11 \times A_{647})] + [34.07 \times (20.78 \times A_{647}) - (4.88 \times A_{664})]\} / 245$  (Wellburn, 1994). Fruit carotenoid extraction was carried out from 20 mg of freeze-dried fruit tissue according to Bianchetti et al., 2018. Phytoene, phytofluene, lycopene,  $\beta$ -carotene, and lutein were determined by high-performance liquid chromatography (HPLC). Eluted compounds were detected at 450 nm (lycopene,  $\beta$ -carotene, and lutein), 286 nm (Phytoene), and 347 nm (Phytofluene) as described in Fraser et al. (2000).

### **Chlorophyll fluorescence measurements**

Chl fluorescence parameters were determined according to Lira et al. (2017) using a portable open gas-exchange system (LI-6400XT system; LI-COR) equipped with an integrated modulated Chl fluorometer (LI-6400-40; LI-COR). Briefly, the second leaflet of the sixth fully expanded leaf from 85-day-old plants was kept under dark adaptation for 60 min, then weak and saturating white light pulses were applied to determine, respectively, initial fluorescence and maximum fluorescence emission. Further, the same procedure was applied on light-adapted leaves to determining the light-adapted initial fluorescence and maximum fluorescence emission. The values were used to calculate maximum quantum efficiency of PSII, PSII operating efficiency, and PSII maximum efficiency.

### **Plastid abundance and ultrastructure**

Two-week-old MoneyMaker and *phyB1B2* plants grown under standard conditions were transferred to the distinct temperature conditions described above. After one week, the fourth fully expanded leaf was used for determining plastid abundance and ultrastructure analysis.

Plastid abundance was determined in the leaf mesophyll as described in Bianchetti et al. (2017). In brief, leaf samples were incubated in 3.5% glutaraldehyde for 60 min and then in 0.1 M Na-EDTA (pH 9.5) at 60°C for 180 min. Isolated cells were visualized through optical microscopy and plastid number per cell was estimated using the ImageJ program (<https://imagej.nih.gov/ij/>).

For ultrastructure analysis, leaf segments were fixed at 4°C in Karnovsky's solution (2.5% [v/v] glutaraldehyde and 2% [v/v] paraformaldehyde in 0.1 M sodium phosphate buffer, pH

7.2) for 24 h. After washing in phosphate buffer, the samples were post-fixed in buffered 1% (w/v) osmium tetroxide, washed, dehydrated in a graded series of acetone, and embedded in Spurr's resin. The resin was polymerized at 60°C. Ultrathin sections were stained with saturated uranyl acetate (Watson, 1958) and lead citrate (Reynolds, 1963) and observed using a JEM 1011 transmission electron microscope.

#### **RNA extraction and reverse transcription quantitative PCR (RT-qPCR)**

RNA extraction, cDNA synthesis, primer design, and qPCR assays were performed as described in Quadrana et al. (2013). The primers used for RT-qPCR analyses are listed in Supplementary Table S2. qPCR reactions were performed in a QStudio6 – A1769 PCR Real-Time thermocycler using 2X Power SYBR Green Master Mix in a final volume of 10 µL. Absolute fluorescence data were analyzed using LinRegPCR software to obtain Ct and primer efficiency values. Relative mRNA abundance was calculated and normalized with the  $\Delta\Delta C_t$  method using two reference genes (Expósito-Rodríguez et al., 2008): *EXPRESSED* and *TIP4.1* for leaves and *EXPRESSED* and *CAC* for fruits (Quadrana et al., 2013).

#### **Phylogenetic analysis**

Amino acid sequences of *A. thaliana* PROTOCHLOROPHYLLIDE OXIDOREDUCTASES (PORA, PORB, and PORC) were BLAST against the tomato genome in Sol Genomics network database (<http://solgenomics.net>). Homologous sequences from *Solanum tuberosum*, *A. thaliana*, *Arapidopsis lyrata*, *Brasica oleracea*, *Brasica rapa*, *Sorghum bicolor*, *Zea mays*, and *Setaria viridis* were retrieved by BLASTp against Viridiplantae in Phytozome (<http://phytozome.jgi.doe.gov/pz/portal.html>). MUSCLE package available in MEGA software 10.0.3 was used to perform multiple sequences alignments. Phylogenetic reconstruction was performed with the maximum-likelihood method with 5,000 bootstrap replications.

#### **Data analysis**

The values in the figures represent the mean of at least three biological replicates  $\pm$  standard error. Statistical differences in parameters were analyzed with InfoStat/F software

(<http://www.infostat.com.ar>). Two-way analysis of variance (ANOVA) was performed to determine genotype (G), environmental (E) or GxE interaction. A Fisher test ( $p < 0.05$ ) was performed to compare GxE interaction and a  $t$ -test ( $p < 0.05$ ) was applied to discriminate means of the sample within genotypes.

#### Accession numbers

Sequence data from this article can be found in the GenBank/EMBL data libraries under accession numbers: AJ001913 (*phyA*); AJ002281 (*phyB1*) and AF122901 (*phyB2*).

#### Supplemental Data

**Supplemental Figure S1.** Time course of temperature and relative humidity measurements registered along the plant growth cycle.

**Supplemental Figure S2.** Hydric status of Moneymaker and knockout-phytochrome mutant plants at two temperatures regimes.

**Supplemental Figure S3.** Phylogenetic construction of the PROTOCHLOROPHYLLIDE OXIDOREDUCTASE protein family.

**Supplemental Figure S4.** PHYTOCHROME INTERACTION FACTORS involvement in the regulation of temperature-induced chlorophyll reduction.

**Supplemental Figure S5.** Expression profile of carotenoid biosynthetic genes in leaves.

**Supplemental Figure S6.** Carotenoid profile in ripe fruits from Moneymaker and knockout- phytochrome mutants.

**Supplemental Figure S7.** Lycopene content in ripe fruits from fruit-specific PHYA- and PHYB2-knockdown transgenic lines.

**Supplemental Table S1.** Relative expression of chlorophyll biosynthetic genes.

**Supplemental Table S2.** Primer sequences used in this study.

#### Figure Legends

**Figure 1. PHYB1/B2 are involved in temperature perception impacting leaf chlorophyll metabolism and fluorescence parameters in tomato.** (A) Side view of 50-day-old *S. lycopersicum* cv. Moneymaker (MM) plants and *phyB1*-, *phyB2*-, and *phyB1B2*-

knockout mutants grown under ambient- (AT, day/night 24°C/18°C) and high-temperature (HT, day/night 30°C/24°C) conditions. (B) Quantification of total chlorophyll (Chl) in the seventh fully expanded leaf from 85-day-old plants. Each bar represents mean  $\pm$  SE. (C) PSII maximum efficiency ( $F_v'/F_m'$ ), PSII operating efficiency ( $F_q'/F_m'$ ), and maximum quantum efficiency of PSII ( $F_v/F_m$ ) measured in the sixth fully expanded leaf from 85-day-old plants.  $n$  = at least five biological replicates. Each bar represents mean  $\pm$  SE. Different letters indicate statistically significant differences according to Fisher's multiple comparison test ( $p < 0.05$ ). Asterisks (\*  $p < 0.05$ , \*\*  $p < 0.01$ ) indicate statistically significant differences by two-tailed Student's  $t$ -test between MM and *phyB1B2* under the same environmental conditions. (D) HT/AT relative expression ratio of *GLK1*, *GGDR*, *CHLG*, *POR1*, *POR2*, and *POR3* mRNA abundance in MM and *phyB1B2*-mutant leaf samples from 85-day-old plants.  $n$  = at least three biological replicates. Each bar represents mean  $\pm$  SE. Asterisks (\*  $p < 0.05$ , \*\*  $p < 0.01$ ) indicate statistically significant differences by two-tailed Student's  $t$ -test between AT and HT within the same genotype. Genes are denoted according to the abbreviations: *GLK1*, *GOLDEN2-LIKE1*; *GGDR*, *GERANYLGERANYL DIPHOSPHATE REDUCTASE*; *CHLG*, *CHLOROPHYLL SYNTHASE*; *POR*, *PROTOCHLOROPHYLLIDE OXIDOREDUCTASE*.

**Figure 2. High temperature affects plastid biogenesis and development in leaves in a PHYB1/B2-dependent manner.** (A) Visualization of a representative leaf from 21-day-old *S. lycopersicum* cv. Moneymaker (MM) and *phyB1B2*-knockout mutants after two weeks under ambient- (AT, day/night 24°C/18°C) and high-temperature (HT, 30°C/24°C) conditions. Red arrows indicate chlorotic leaves (MM at HT, *phyB1B2* at AT, and *phyB1B2* at HT). (B) Quantification of total Chl in leaves cultivated under AT (blue background) and HT (yellow background) conditions.  $n$  = at least three biological replicates. Each bar represents mean  $\pm$  SE. (C) Plastid density per mesophyll cell. Values represent chloroplast quantification of  $\pm 70$  cells. Different letters indicate statistically significant differences according to Fisher's multiple comparison test ( $p < 0.05$ ). Each bar represents mean  $\pm$  SE. (D) Representative TEM images of chloroplasts from MM and *phyB1B2* leaves grown under AT and HT conditions. G indicates grana and DT indicates dilated thylakoids.

**Figure 3. High temperature enhances chlorophyll degradation in leaves in a PHYB1/B2-dependent manner.** (A) Schematic model of chlorophyll (Chl) degradation pathway. Enzymes and metabolites are denoted according to the following abbreviations: Pheo *a*, pheophytin *a*; Chlide *a*, chlorophyllide *a*; Pheide *a*, pheophorbide *a*; RCC, red chlorophyll catabolite; CLH, CHLOROPHYLLASE; SGR, STAY GREEN; SGR-like, PPH, PHEOPHYTINASE; STAY GREEN-LIKE; PAO, PHEOPHORBIDE *a* OXYGENASE. The enzymes highlighted in red are those that showed to be regulated by temperature in a PHYB1/B2-dependent manner according to Figure 3B. (B) Relative mRNA levels of Chl degrading enzyme-encoding genes in Moneymaker (MM) and *phyB1B2* mutant leaf samples from 85-day-old plants grown under ambient- (AT, 24°C/18°C; blue background) and high-temperature (HT, 30°C/24°C; yellow background) conditions. Expression levels are relative to MM – AT conditions. *n* = at least three biological replicates. Each bar represents mean ± SE. Different letters indicate statistically significant differences according to Fisher's multiple comparison test (*p* < 0.05).

**Figure 4. PHYB1/B2-dependent temperature perception transcriptionally regulates leaf carotenogenesis.** (A) Total carotenoid levels expressed in µg per g of dry weight. *n* = at least five biological replicates. (B) Relative mRNA levels of *GGPS1* gene in Moneymaker (MM) and *phyB1B2*-mutant leaf samples from 85-day-old plants grown under ambient- (AT, 24°C/18°C; blue background) and high-temperature (HT, 30°C/24°C; yellow background) conditions. Expression levels are relative to MM – AT conditions. *n* = at least three biological replicates. Each bar represents mean ± SE. Different letters indicate statistically significant differences according to Fisher's multiple comparison test (*p* < 0.05). Gene is denoted according to the abbreviation: *GGPS1*, *GERANYLGERANYL PHOSPHATE SYNTHASE 1*.

**Figure 5. PHYA/B1/B2-dependent temperature perception transcriptionally regulates fruit carotenogenesis.** (A) Total carotenoid (phytoene, phytofluene, lycopene, lutein, and β-carotene) levels quantified from ripe fruits of Moneymaker (MM) and *phyA*-, *phyB1*-, *phyB2*-, *phyB1B2*-, and *phyAB1B2*-mutant plants grown under ambient- (AT, day/night

24°C/18°C; blue fill) and high-temperature (HT, day/night 30°C/24°C; yellow fill) conditions. (B) Center: schematic model of the lycopene biosynthetic pathway, the dotted line represents more than one enzymatic step. Left: levels of lycopene, phytoene, and phytofluene in ripe fruits. AT: blue background; HT: yellow background. Each bar represents mean  $\pm$  SE. Different letters indicate statistically significant differences according to Fisher's multiple comparison test ( $p < 0.05$ ). Right: Relative mRNA levels of carotenoid biosynthetic genes *GGPS2*, *PSY1*, and *PDS* in fruits at mature green (MG) and breaker (BK) stages harvested from plants grown under AT (blue) and HT (yellow) conditions. Transcripts levels are expressed relative to MM MG – AT condition. Asterisks (\*  $p < 0.05$ , \*\*  $p < 0.01$ ) indicate differences in the analysis of variance in a multiple comparison test within the same fruit stage. Metabolites and genes are denoted according to the following abbreviations: GGDP, geranylgeranyl diphosphate; *GGPS2*, *GERANYLGERANYL PHOSPHATE SYNTHASE 2*; *PSY1*, *PHYTOENE SYNTHASE 1*; *PDS*, *PHYTOENE DESATURASE*. (C) Relative mRNA levels of *PIF1a* carotenogenesis regulator gene in fruits at mature green (MG) and breaker (BK) stages harvested from plants grown under AT (blue) and HT (yellow) conditions. Transcripts levels are expressed relative to MM MG – AT conditions. Asterisks (\*\*  $p < 0.01$ ) indicate differences in the analysis of variance in a multiple comparison test within the same fruit stage.

**Figure 6. Fruit-localized PHYA and PHYB2 are involved in temperature perception impacting lycopene synthesis and master fruit ripening regulators.** (A) Lycopene levels quantified in ripe fruits from Micro-Tom (MT) control genotype and fruit-specific *PHYA*- (*PHYA*<sup>RNAi</sup>) and *PHYB2*- (*PHYB2*<sup>RNAi</sup>) knockdown transgenic lines grown under ambient- (24°C/18°C) and high-temperature (30°C/24°C) conditions. Lycopene levels were quantified and expressed relative to MT fruits under AT conditions and values are means of at least three biological replicates from two independent lines for each genotype. Each bar represents mean  $\pm$  SE. (B,C) Relative mRNA levels of (B) *PSY1* (C) and master fruit ripening regulator genes in MT, *PHYA*<sup>RNAi</sup>, and *PHYB2*<sup>RNAi</sup> breaker fruit samples harvested under AT and HT conditions. Expression levels are relative to MT – AT conditions. n = at least three biological replicates. Each bar represents mean  $\pm$  SE. Different letters indicate statistically significant differences according to Fisher's multiple comparison test ( $p <$

0.05). *RIN*; *RIPENING INHIBITOR*, *NOR*; *NON-RIPENING*, *FUL1*; *FRUITFULL1*, *FUL2*;  
*FRUITFULL2*, *AP2a*; *APETALA2a*, *TAGL1*; *TOMATO AGAMOUS-LIKE1*, *PSY1*;  
*PHYTOENE SYNTHASE 1*.

**Figure 7. The effect of PHY-mediated temperature perception on tomato metabolism regulation.** The rise of ambient temperature shifts balance to the inactive phytochrome (Pr) form, which promotes the Chl degradation pathway in source leaves through the transcriptional up-regulation of Chl catabolic enzyme-associated genes. Additionally, reduced levels of Pfr impair carotenoid accumulation in both leaves and ripe fruits, through the transcriptional downregulation of carotenoid biosynthetic and master ripening regulator genes.

## Parsed Citations

**Alba R, Cordonnier-Pratt MM, Pratt LH. (2000a).** Fruit-localized phytochromes regulate lycopene accumulation independently of ethylene production in tomato. *Plant Physiology* 123: 363–370.

Pubmed: [Author and Title](#)

Google Scholar: [Author Only](#) [Title Only](#) [Author and Title](#)

**Alba R, Kelmenson PM, Cordonnier-Pratt MM, Pratt LH. (2000b).** The phytochrome gene family in tomato and the rapid differential evolution of this family in angiosperms. *Molecular Biology and Evolution* 17: 362–373.

Pubmed: [Author and Title](#)

Google Scholar: [Author Only](#) [Title Only](#) [Author and Title](#)

**Almeida J, Asís R, Molineri VN, Sestari I, Lira BS, Carrari F, Peres LEP, Rossi M. (2015).** Fruits from ripening impaired, chlorophyll degraded and jasmonate insensitive tomato mutants have altered tocopherol content and composition. *Phytochemistry* 111: 72–83.

Pubmed: [Author and Title](#)

Google Scholar: [Author Only](#) [Title Only](#) [Author and Title](#)

**Alves FRR, Lira BS, Pikart FC, Monteiro SS, Furlan CM, Purgatto E, Pascoal GB, Andrade SCS, Demarco D, Rossi M, Freschi L. (2020).** Beyond the limits of photoperception: constitutively active PHYTOCHROME B2 overexpression as a means of improving fruit nutritional quality in tomato. *Plant Biotechnology Journal* <https://doi.org/10.1111/pbi.13362>.

Pubmed: [Author and Title](#)

Google Scholar: [Author Only](#) [Title Only](#) [Author and Title](#)

**Ayenan MAT, Danquah A, Hanson P, Ampomah-Dwamena C, Sodedji FAK, Asante IK, Danquah EY. (2019)** Accelerating Breeding for Heat Tolerance in Tomato (*Solanum lycopersicum* L.: An Integrated Approach. *Agronomy* 9: 720.

Pubmed: [Author and Title](#)

Google Scholar: [Author Only](#) [Title Only](#) [Author and Title](#)

**Bianchetti RE, Cruz AB, Oliveira BS, Demarco D, Purgatto E, Peres LEP, Rossi M, Freschi L. (2017).** Phytochromobilin deficiency impairs sugar metabolism through the regulation of cytokinin and auxin signaling in tomato fruits. *Scientific Reports* 7: 7822.

Pubmed: [Author and Title](#)

Google Scholar: [Author Only](#) [Title Only](#) [Author and Title](#)

**Bianchetti RE, Lira BS, Monteiro SS, Demarco D, Purgatto E, Rothan C, Rossi M, Freschi L. (2018).** Fruit-localized phytochromes regulate plastid biogenesis, starch synthesis, and carotenoid metabolism in tomato. *Journal of Experimental Botany* 69: 3573–3586.

Pubmed: [Author and Title](#)

Google Scholar: [Author Only](#) [Title Only](#) [Author and Title](#)

**Bitá CE, Gerats T. (2013).** Plant tolerance to high temperature in a changing environment: scientific fundamentals and production of heat stress-tolerant crops. *Frontiers in Plant Science* 4: 273.

Pubmed: [Author and Title](#)

Google Scholar: [Author Only](#) [Title Only](#) [Author and Title](#)

**Box MS, Huang BE, Domijan M, Jaeger KE, Khattak AK, Yoo SJ, Sedivey EL, Jones DM, Hearn TJ, Webb ARR, Grant A, Locke JCW, Wigge PA. (2015).** ELF3 controls thermoresponsive growth in *Arabidopsis*. *Current Biology* 25: 194–199.

Pubmed: [Author and Title](#)

Google Scholar: [Author Only](#) [Title Only](#) [Author and Title](#)

**Burgie ES, Vierstra RD. (2014).** Phytochromes: An Atomic Perspective on Photoactivation and Signaling. 26: 4568–4583.

Pubmed: [Author and Title](#)

Google Scholar: [Author Only](#) [Title Only](#) [Author and Title](#)

**Campos ML, Carvalho RF, Benedito VA, Peres LEP. (2010).** The Micro-Tom model system as a tool to discover novel hormonal functions and interactions. *Plant Signaling & Behavior* 5: 267–270.

Pubmed: [Author and Title](#)

Google Scholar: [Author Only](#) [Title Only](#) [Author and Title](#)

**Chung MY, Vrebalov J, Alba R, Lee J, McQuinn R, Chung JD, Klein P, Giovannoni J. (2010).** A tomato (*Solanum lycopersicum*) APETALA2/ERF gene, SIAP2a, is a negative regulator of fruit ripening. *Plant Journal* 64: 936–947.

Pubmed: [Author and Title](#)

Google Scholar: [Author Only](#) [Title Only](#) [Author and Title](#)

**Cordoba E, Salmi M, León P. (2009).** Unravelling the regulatory mechanisms that modulate the MEP pathway in higher plants. *Journal of Experimental Botany* 60: 2933–2943.

Pubmed: [Author and Title](#)

Google Scholar: [Author Only](#) [Title Only](#) [Author and Title](#)

**Cruz AB, Bianchetti RE, Alves FRR, Purgatto E, Peres LEP, Rossi M, Freschi L. 2018.** Light, Ethylene and Auxin Signaling Interaction Regulates Carotenoid Biosynthesis During Tomato Fruit Ripening. *Frontiers in Plant Science* 9: 1370.

Pubmed: [Author and Title](#)

Google Scholar: [Author Only](#) [Title Only](#) [Author and Title](#)

**Dubreuil C, Ji Y, Strand Å, Grönlund A. (2017).** A quantitative model of the phytochrome-PIF light signalling initiating chloroplast development. *Scientific Reports* 7: 13684.

Downloaded from on May 14, 2020 - Published by www.plantphysiol.org  
Copyright © 2020 American Society of Plant Biologists. All rights reserved.



Pubmed: [Author and Title](#)  
Google Scholar: [Author Only](#) [Title Only](#) [Author and Title](#)

**Expósito-Rodríguez M, Borges AA, Borges-Pérez A, Pérez JA. (2008). Selection of internal control genes for quantitative real-time RT-PCR studies during tomato development process. BMC Plant Biology 8: 131.**

Pubmed: [Author and Title](#)  
Google Scholar: [Author Only](#) [Title Only](#) [Author and Title](#)

**Fahad S, Bajwa AA, Nazir U, Anjum SA, Farooq A, Zohaib A, Sadia S, Nasim W, Adkins S, Saud S, Ihsan MZ, Alharby H, Wu C, Wang D, Huang J. (2017). Crop Production under Drought and Heat Stress: Plant Responses and Management Options. Frontiers in Plant Science. 8: 1147.**

Pubmed: [Author and Title](#)  
Google Scholar: [Author Only](#) [Title Only](#) [Author and Title](#)

**Fraser PD, Pinto M, Holloway DE, Bramley P. (2000). Application of high-performance liquid chromatography with photodiode array detection to the metabolic profiling of plant isoprenoids. The Plant Journal 24: 551-558.**

Pubmed: [Author and Title](#)  
Google Scholar: [Author Only](#) [Title Only](#) [Author and Title](#)

**Fujii Y, Tanaka H, Konno N, Ogasawara Y, Hamashima N, Tamura S, Hasegawa S, Hayasaki Y, Okajima K, Kodama T. (2017). Phototropin perceives temperature based on the lifetime of its photoactivated state. Proceedings of the National Academy of Sciences 114: 9206–9211.**

Pubmed: [Author and Title](#)  
Google Scholar: [Author Only](#) [Title Only](#) [Author and Title](#)

**Gramegna G, Rosado D, Carranza APS, Cruz AB, Simon-Moya M, Llorente B, Rodríguez-Concepción, M, Freschi L, Rossi M. (2018). PHYTOCHROME - INTERACTING FACTOR 3 mediates light - dependent induction of tocopherol biosynthesis during tomato fruit ripening. Plant Cell & Environment 42: 1328–1399.**

Pubmed: [Author and Title](#)  
Google Scholar: [Author Only](#) [Title Only](#) [Author and Title](#)

**Gupta SK, Sharma S, Santisree P, Kilambi HV, Appenroth K, Sreelakshmi Y, Sharma R. (2014). Complex and shifting interactions of phytochromes regulate fruit development in tomato. Plant, Cell and Environment 37: 1688–1702.**

Pubmed: [Author and Title](#)  
Google Scholar: [Author Only](#) [Title Only](#) [Author and Title](#)

**Guyer L, Hofstetter SS, Christ B, Lira BS, Rossi M, Hörtensteiner S. (2014). Different Mechanisms Are Responsible for Chlorophyll Dephytylation during Fruit Ripening and Leaf Senescence in Tomato. Plant Physiology 166: 44–56.**

Pubmed: [Author and Title](#)  
Google Scholar: [Author Only](#) [Title Only](#) [Author and Title](#)

**Hörtensteiner S. (2013). Update on the biochemistry of chlorophyll breakdown. Plant Molecular Biology 82: 505–517.**

Pubmed: [Author and Title](#)  
Google Scholar: [Author Only](#) [Title Only](#) [Author and Title](#)

**Huang H, McLoughlin KE, Sorkin ML, Burgie ES, Bindbeutel RK, Vierstra RD, Nusinow DA. (2019). PCH1 regulates light, temperature, and circadian signaling as a structural component of phytochrome B-photobodies in Arabidopsis. Proceedings of the National Academy of Sciences 116: 8603–8608.**

Pubmed: [Author and Title](#)  
Google Scholar: [Author Only](#) [Title Only](#) [Author and Title](#)

**Inagaki N, Kinoshita K, Kagawa T, Tanaka A, Ueno O, Shimada H, Takano M. (2015). Phytochrome B Mediates the Regulation of Chlorophyll Biosynthesis through Transcriptional Regulation of ChlH and GUN4 in Rice Seedlings. PLoS ONE 10: 10.1371/journal.pone.0135408.**

Pubmed: [Author and Title](#)  
Google Scholar: [Author Only](#) [Title Only](#) [Author and Title](#)

**Ishida A, Toma T, Marjenah M. (2000) Leaf gas exchange and canopy structure under wet and drought years in Macaranga conifera, a tropical pioneer tree. Rainforest Ecosystems of East Kalimantan 140:129-42.**

Pubmed: [Author and Title](#)  
Google Scholar: [Author Only](#) [Title Only](#) [Author and Title](#)

**Jung JH, Domijan M, Klose C, Biswas S, Ezer D, Gao M, Khattak AK, Box MS, Charoensawan V, Cortijo S, Kumar M, Grant A, Locke JC, Schäfer E, Jaeger KE, Wigge PA. (2016). Phytochromes function as thermosensors in Arabidopsis. Science 354: 886–889.**

Pubmed: [Author and Title](#)  
Google Scholar: [Author Only](#) [Title Only](#) [Author and Title](#)

**Karlova R, Rosin FM, Busscher-Lange J, Parapunova V, Do PT, Fernie AR, Fraser PD, Baxter C, Angenent GC, de Maagd RA. (2011). Transcriptome and Metabolite Profiling Show That APETALA2a Is a Major Regulator of Tomato Fruit Ripening. The Plant Cell 23: 923–941.**

Pubmed: [Author and Title](#)  
Google Scholar: [Author Only](#) [Title Only](#) [Author and Title](#)

**Kerckhoffs LHJ, Kelmenson PM, Schreuder MEL, Kendrick CI, Kendrick RE, Hanhart CJ, Koornneef M, Pratt LH, Cordonnier-Pratt MM.**

Downloaded from on May 14, 2020 - Published by www.plantphysiol.org  
Copyright © 2020 American Society of Plant Biologists. All rights reserved.

(1999). Characterization of the gene encoding the apoprotein of phytochrome B2 in tomato, and identification of molecular lesions in two mutant alleles. *Molecular and General Genetics* 261: 901–907.

Pubmed: [Author and Title](#)

Google Scholar: [Author Only](#) [Title Only](#) [Author and Title](#)

Kerckhoffs LHJ, Schreuder MEL, VanTuinen A, Koornneef M, Kendrick RE. (1997). Phytochrome control of anthocyanin biosynthesis in tomato seedlings: Analysis using photomorphogenic mutants. *Photochemistry and Photobiology* 65: 374–381.

Pubmed: [Author and Title](#)

Google Scholar: [Author Only](#) [Title Only](#) [Author and Title](#)

Kerckhoffs LHJ, Van Tuinen A, Hauser BA, Cordonnier Pratt MM, Nagatani A, Koornneef M, Pratt LH, Kendrick RE. (1996). Molecular analysis of tri-mutant alleles in tomato indicates the Tri locus is the gene encoding the apoprotein of phytochrome B1. *Planta* 199: 152–157.

Pubmed: [Author and Title](#)

Google Scholar: [Author Only](#) [Title Only](#) [Author and Title](#)

Kim K, Jeong J, Kim J, Lee N, Kim ME, Lee S, Kim SC, Choi G. (2016). PIF1 regulates plastid development by repressing photosynthetic genes in the endodermis. *Mol. Plant* 9: 1415–1427

Pubmed: [Author and Title](#)

Google Scholar: [Author Only](#) [Title Only](#) [Author and Title](#)

Klee HJ, Giovannoni JJ. (2011). Genetics and Control of Tomato Fruit Ripening and Quality Attributes. *Annual Review of Genetics* 45: 41–59.

Pubmed: [Author and Title](#)

Google Scholar: [Author Only](#) [Title Only](#) [Author and Title](#)

Koini MA, Alvey L, Allen T, Tilley CA, Harberd NP, Whitlam GC, Franklin KA. (2009). Report High Temperature-Mediated Adaptations in Plant Architecture Require the bHLH Transcription Factor PIF4. *Current Biology* 19: 408–413.

Pubmed: [Author and Title](#)

Google Scholar: [Author Only](#) [Title Only](#) [Author and Title](#)

Lazarova GI, Kerckhoffs LHJ, Brandstädter J, Matsui M, Kendrick RE, Cordonnier-Pratt MM, Pratt LH. (1998a). Molecular analysis of PHYA in wild-type and phytochrome A-deficient mutants of tomato. *Plant Journal* 14: 653–662.

Pubmed: [Author and Title](#)

Google Scholar: [Author Only](#) [Title Only](#) [Author and Title](#)

Lazarova GI, Kubota T, Frances S, Peters JL, Hughes MJ, Brandstadter J, Széll M, Matsui M, Kendrick RE, Cordonnier-Pratt MM, Pratt LH. (1998b). Characterization of tomato PHYB1 and identification of molecular defects in four mutant alleles. *Plant Molecular Biology* 38: 1137–1146.

Pubmed: [Author and Title](#)

Google Scholar: [Author Only](#) [Title Only](#) [Author and Title](#)

Legris M, Klose C, Burgie ES, Rojas CCR, Neme M, Hiltbrunner A, Wigge PA, Schäfer E, Vierstra RD, Casal JJ. (2016). Phytochrome B integrates light and temperature signals in Arabidopsis. *Science* 354: 897–900.

Pubmed: [Author and Title](#)

Google Scholar: [Author Only](#) [Title Only](#) [Author and Title](#)

Legris M, Nieto C, Sellaro R, Prat S, Casal JJ. (2017). Perception and signalling of light and temperature cues in plants. *Plant Journal* 90: 683–697.

Pubmed: [Author and Title](#)

Google Scholar: [Author Only](#) [Title Only](#) [Author and Title](#)

Lira BS, Gramegna G, Trench B, Alves FRR, Silva EM, Silva GFF, Thirulmalaikumar VP, Lupi ACD, Demarco D, Purgatto E, Nogueira FTS, Balazadeh S, Freschi L, Rossi M. (2017). Manipulation of a senescence-associated gene improves fleshy fruit yield. *Plant Physiology* 175: 77–91.

Pubmed: [Author and Title](#)

Google Scholar: [Author Only](#) [Title Only](#) [Author and Title](#)

Lira BS, de Setta N, Rosado D, Almeida J, Freschi L, Rossi M. (2014). Plant degreening: Evolution and expression of tomato (*Solanum lycopersicum*) dephytylation enzymes. *Gene* 546: 359–366.

Pubmed: [Author and Title](#)

Google Scholar: [Author Only](#) [Title Only](#) [Author and Title](#)

Liu L, Shao Z, Zhang M, Wang Q. (2015). Regulation of carotenoid metabolism in tomato. *Molecular Plant* 8: 28–39.

Pubmed: [Author and Title](#)

Google Scholar: [Author Only](#) [Title Only](#) [Author and Title](#)

Llorente B, D'Andrea L, Ruiz-Sola MA, Botterweg E, Pulido P, Andilla J, Loza-Alvarez P, Rodriguez-Concepcion M. (2016). Tomato fruit carotenoid biosynthesis is adjusted to actual ripening progression by a light-dependent mechanism. *Plant Journal* 85: 107–119.

Pubmed: [Author and Title](#)

Google Scholar: [Author Only](#) [Title Only](#) [Author and Title](#)

Lorrain S, Allen T, Duek PD, Whitlam GC, Fankhauser C. (2008). Phytochrome-mediated inhibition of shade avoidance involves degradation of growth-promoting bHLH transcription factors. *Plant Journal* 53: 312–323.

Downloaded from on May 14, 2020 - Published by [www.plantphysiol.org](http://www.plantphysiol.org)  
Copyright © 2020 American Society of Plant Biologists. All rights reserved.

Pubmed: [Author and Title](#)  
Google Scholar: [Author Only](#) [Title Only](#) [Author and Title](#)

**Ma D, Li X, Guo Y, Chu J, Fang S, Yan C, Noel JP, Liu H. (2016). Cryptochrome 1 interacts with PIF4 to regulate high temperature-mediated hypocotyl elongation in response to blue light. *Proceedings of the National Academy of Sciences* 113: 224–229.**

Pubmed: [Author and Title](#)  
Google Scholar: [Author Only](#) [Title Only](#) [Author and Title](#)

**Martin G, Leivar P, Ludevid D, Tepperman JM, Quail PH, Monte E. (2016). Phytochrome and retrograde signalling pathways converge to antagonistically regulate a light-induced transcriptional network. *Nature Communications* 7: 11431.**

Pubmed: [Author and Title](#)  
Google Scholar: [Author Only](#) [Title Only](#) [Author and Title](#)

**Martínez-García JF, Huq E, Quail PH. (2000). Direct Targeting of Light Signals to a Promoter. *Science* 288: 859–859.**

Pubmed: [Author and Title](#)  
Google Scholar: [Author Only](#) [Title Only](#) [Author and Title](#)

**Nakamura H, Muramatsu M, Hakata M, Ueno O, Nagamura Y, Hirochika H, Takano M, Ichikawa H, (2009). Ectopic overexpression of the transcription factor OsGLK1 induces chloroplast development in non-green rice cells. *Plant Cell Physiology* 50: 1933–1949.**

Pubmed: [Author and Title](#)  
Google Scholar: [Author Only](#) [Title Only](#) [Author and Title](#)

**Nguyen C V, Vrebalov JT, Gapper NE, Zheng Y, Zhong S, Fei Z, Giovannoni JJ. (2014). Tomato GOLDEN2-LIKE Transcription Factors Reveal Molecular Gradients That Function during Fruit Development and Ripening. *Plant Cell* 26: 585–601.**

Pubmed: [Author and Title](#)  
Google Scholar: [Author Only](#) [Title Only](#) [Author and Title](#)

**Oh S, Montgomery BL. (2014). Phytochrome-dependent coordinate control of distinct aspects of nuclear and plastid gene expression during anterograde signaling and photomorphogenesis. *Frontiers in Plant Science* 5: 171.**

Pubmed: [Author and Title](#)  
Google Scholar: [Author Only](#) [Title Only](#) [Author and Title](#)

**Park E, Kim Y, Choi G. (2018). Phytochrome B Requires PIF Degradation and Sequestration to Induce Light Responses across a Wide Range of Light Conditions. *Plant Cell* 30: 1277–1292.**

Pubmed: [Author and Title](#)  
Google Scholar: [Author Only](#) [Title Only](#) [Author and Title](#)

**Qiu Y, Li M, Kim RJ, Moore CM, Chen M. (2019). Daytime temperature is sensed by phytochrome. *Nature Communications* 10: 140.**

Pubmed: [Author and Title](#)  
Google Scholar: [Author Only](#) [Title Only](#) [Author and Title](#)

**Quadrana L, Almeida J, Otaiza SN, Duffy T, Corrêa da Silva JV, de Godoy F, Asís R, Bermúdez L, Fernie AR, Carrari F, Rossi M. (2013). Transcriptional regulation of tocopherol biosynthesis in tomato. *Plant Molecular Biology* 81: 309–325.**

Pubmed: [Author and Title](#)  
Google Scholar: [Author Only](#) [Title Only](#) [Author and Title](#)

**Reynolds ES. (1963). The use of lead citrate at high pH as an electron-opaque stain in electron microscopy. *The Journal of Cell Biology* 17: 208–212.**

Pubmed: [Author and Title](#)  
Google Scholar: [Author Only](#) [Title Only](#) [Author and Title](#)

**Rockwell NC, Su Y-S, Lagarias JC. (2006). Phytochrome Structure and Signaling Mechanisms. *Annual Review of Plant Biology* 57: 837–858.**

Pubmed: [Author and Title](#)  
Google Scholar: [Author Only](#) [Title Only](#) [Author and Title](#)

**Rosado D, Gramegna G, Cruz A, Lira BS, Freschi L, De Setta N, Rossi M. (2016). Phytochrome Interacting Factors (PIFs) in *Solanum lycopersicum*: Diversity, evolutionary history and expression profiling during different developmental processes. *PLoS ONE* 11: 10.1371/journal.pone.0165929.**

Pubmed: [Author and Title](#)  
Google Scholar: [Author Only](#) [Title Only](#) [Author and Title](#)

**Rosado D, Trench B, Bianchetti R, Zuccarelli R, Alves FRR, Purgatto E, Floh EIS, Nogueira FTS, Freschi L, Rossi M. (2019). Downregulation of PHYTOCHROME-INTERACTING FACTOR 4 influences plant development and fruit production. *Plant Physiology* 181: 1360–1370.**

Pubmed: [Author and Title](#)  
Google Scholar: [Author Only](#) [Title Only](#) [Author and Title](#)

**Saidi Y, Finka A, Goloubinoff, P. (2017). Heat perception and signalling in plants: a tortuous path to thermotolerance. *New Phytologist* 190: 556–565.**

Pubmed: [Author and Title](#)  
Google Scholar: [Author Only](#) [Title Only](#) [Author and Title](#)

**Sakuraba Y, Jeong J, Kang MY, Kim J, Paek NC, Choi G. (2014). Phytochrome-interacting transcription factors PIF4 and PIF5 induce leaf senescence in *Arabidopsis*. *Nature Communications* 5: 4636.**

Pubmed: [Author and Title](#)  
Google Scholar: [Author Only](#) [Title Only](#) [Author and Title](#)

**Sharrock RA, Quail PH. (1989). Novel phytochrome sequences in *Arabidopsis thaliana*: structure, evolution, and differential expression of a plant regulatory photoreceptor family. *Genes & Development* 3: 1745–1757.**

Pubmed: [Author and Title](#)  
Google Scholar: [Author Only](#) [Title Only](#) [Author and Title](#)

**Sims DA, Gamon JA (2003). Estimation of vegetation water content and photosynthetic tissue area from spectral reflectance: a comparison of indices based on liquid water and chlorophyll absorption features. *Remote Sensing of Environment* 84: 526–537.**

Pubmed: [Author and Title](#)  
Google Scholar: [Author Only](#) [Title Only](#) [Author and Title](#)

**Song Y, Yang C, Gao S, Zhang W, Li L, Kuai B. (2014). Age-triggered and dark-induced leaf senescence requires the bHLH transcription factors PIF3,4, and 5. *Molecular Plant* 7: 1776–1787.**

Pubmed: [Author and Title](#)  
Google Scholar: [Author Only](#) [Title Only](#) [Author and Title](#)

**Spicher L, Almeida J, Gutbrod K, Pipitone R, Dörmann P, Glauser G, Rossi M, Kessler F. (2017). Essential role for phytol kinase and tocopherol in tolerance to combined light and temperature stress in tomato. *Journal of Experimental Botany* 68: 5845–5856.**

Pubmed: [Author and Title](#)  
Google Scholar: [Author Only](#) [Title Only](#) [Author and Title](#)

**Spicher L, Glauser G, Kessler F. (2016). Lipid Antioxidant and Galactolipid Remodeling under Temperature Stress in Tomato Plants. *Frontiers in Plant Science* 7: 167.**

Pubmed: [Author and Title](#)  
Google Scholar: [Author Only](#) [Title Only](#) [Author and Title](#)

**Stephenson PG, Fankhauser C, Terry MJ. (2009). PIF3 is a repressor of chloroplast development. *Proceedings of the National Academy of Sciences* 106: 7654–7659.**

Pubmed: [Author and Title](#)  
Google Scholar: [Author Only](#) [Title Only](#) [Author and Title](#)

**Suwa R, Hakata H, Hara H, El-Shemy HA, Adu-Gyamfi JJ, Nguyen NT, Kanai S, Lightfoot DA, Mohapatra PK, Fujita K. (2010). High temperature effects on photosynthate partitioning and sugar metabolism during ear expansion in maize (*Zea mays* L.) genotypes. *Plant Physiology and Biochemistry* 48: 124–130.**

Pubmed: [Author and Title](#)  
Google Scholar: [Author Only](#) [Title Only](#) [Author and Title](#)

**Takahashi S, Murata N. (2008). How do environmental stresses accelerate photoinhibition? *Trends in Plant Science* 13: 178–182.**

Pubmed: [Author and Title](#)  
Google Scholar: [Author Only](#) [Title Only](#) [Author and Title](#)

**Toledo-Ortiz G, Johansson H, Lee KP, Bou-torrent J, Stewart K, Steel G, Rodríguez-Concepción M, Halliday KJ. (2014). The HY5-PIF Regulatory Module Coordinates Light and Temperature Control of Photosynthetic Gene Transcription. *PLoS Genetics* 10: 10.1371/journal.pgen.1004416.**

Pubmed: [Author and Title](#)  
Google Scholar: [Author Only](#) [Title Only](#) [Author and Title](#)

**Tomato Genome Consortium. (2012). The tomato genome sequence provides insights into fleshy fruit evolution. *Nature* 485: 635–641.**

Pubmed: [Author and Title](#)  
Google Scholar: [Author Only](#) [Title Only](#) [Author and Title](#)

**Van Eerden FJ, De Jong DH, De Vries AH, Wassenaar TA, Marrink SJ. (2015). Characterization of thylakoid lipid membranes from cyanobacteria and higher plants by molecular dynamics simulations. *Biochimica et Biophysica Acta - Biomembranes* 1848: 1319–1330.**

Pubmed: [Author and Title](#)  
Google Scholar: [Author Only](#) [Title Only](#) [Author and Title](#)

**Velikova V, Varkonyi Z, Szabo M, Maslenkova L, Nogues I, Kóvacs L, Peeva V, Busheva M, Garab G, Sharkey TD, Loreto F. (2011). Increased Thermostability of Thylakoid Membranes in Isoprene-Emitting Leaves Probed with Three Biophysical Techniques. *Plant Physiology* 157: 905–916.**

Pubmed: [Author and Title](#)  
Google Scholar: [Author Only](#) [Title Only](#) [Author and Title](#)

**Watson ML. (1958). Staining of Tissue Sections for Electron Microscopy with Heavy Metals: II. Application of Solutions Containing Lead and Barium. *The Journal of Cell Biology* 25: 727–730.**

Pubmed: [Author and Title](#)  
Google Scholar: [Author Only](#) [Title Only](#) [Author and Title](#)

**Wellburn A. (1994). The spectral determination of chlorophylls a and b, as well as total carotenoids, using various solvents with spectrophotometers of different resolution. *Journal of Plant Physiology* 144: 307–313.**

Pubmed: [Author and Title](#)  
Google Scholar: [Author Only](#) [Title Only](#) [Author and Title](#)

**Weller JL, Schreuder MEL, Smith H, Koorneef M, Kendrick RE. (2000). Physiological interactions of phytochromes A, B1 and B2 in the**

control of development in tomato. *Plant Journal* 24: 345–356.

Pubmed: [Author and Title](#)

Google Scholar: [Author Only](#) [Title Only](#) [Author and Title](#)

Yamori W, von Caemmerer S. (2009). Effect of Rubisco Activase Deficiency on the Temperature Response of CO<sub>2</sub> Assimilation Rate and Rubisco Activation State: Insights from Transgenic Tobacco with Reduced Amounts of Rubisco Activase. *Plant Physiology* 151: 2073–2082.

Pubmed: [Author and Title](#)

Google Scholar: [Author Only](#) [Title Only](#) [Author and Title](#)

Yuan XY, Wang RH, Zhao XD, Luo YB, Fu DQ. (2016). Role of the tomato Non-Ripening mutation in regulating fruit quality elucidated using iTRAQ protein profile analysis. *PLoS ONE* 11: 10.1371/journal.pone.0164335.

Pubmed: [Author and Title](#)

Google Scholar: [Author Only](#) [Title Only](#) [Author and Title](#)

Zhang Y, Liu Z, Chen Y, He, J, Bi Y. (2015). PHYTOCHROME-INTERACTING FACTOR 5 (PIF5) positively regulates dark-induced senescence and chlorophyll degradation in *Arabidopsis*. *Plant Science* 237: 57–68.

Pubmed: [Author and Title](#)

Google Scholar: [Author Only](#) [Title Only](#) [Author and Title](#)

Zhang Y, Mayba O, Pfeiffer A, Shi H, Tepperman JM, Speed TP, Quail PH. (2013). A Quartet of PIF bHLH Factors Provides a Transcriptionally Centered Signaling Hub That Regulates Seedling Morphogenesis through Differential Expression-Patterning of Shared Target Genes in *Arabidopsis*. *PLoS Genetics* 9: 10.1371/journal.pgen.1003244.

Pubmed: [Author and Title](#)

Google Scholar: [Author Only](#) [Title Only](#) [Author and Title](#)

Zhang R, Sharkey TD. (2009). Photosynthetic electron transport and proton flux under moderate heat stress. *Photosynthesis Research* 100: 29–43.

Pubmed: [Author and Title](#)

Google Scholar: [Author Only](#) [Title Only](#) [Author and Title](#)

Zhao C, Liu B, Piao S, Wang X, Lobell DB, Huang Y, Huang M, Yao Y, Bassu S, Ciais P, Durand JL, Elliott J, Ewert F, Janssens IA, Li T, Lin E, Liu Q, Martre P, Müller C, Peng S, Peñuelas J, Ruane AC, Wallach D, Wang T, Wu D, Liu Z, Zhu Y, Zhu Z, Asseng S. (2017). Temperature increase reduces global yields of major crops in four independent estimates. *Proceedings of the National Academy of Sciences* 114: 9326–9331.

Pubmed: [Author and Title](#)

Google Scholar: [Author Only](#) [Title Only](#) [Author and Title](#)

Zhao F, Zhang D, Zhao Y, Wang W, Yang H, Tai F, Li C, Hu X. (2016). The Difference of Physiological and Proteomic Changes in Maize Leaves Adaptation to Drought, Heat, and Combined Both Stresses. *Frontiers in Plant Science* 7: 1471.

Pubmed: [Author and Title](#)

Google Scholar: [Author Only](#) [Title Only](#) [Author and Title](#)

Zhou Y, Xun Q, Zhang D, Lv M, Ou Y, Li J. (2019). TCP Transcription Factors Associate with PHYTOCHROME INTERACTING FACTOR 4 and CRYPTOCHROME 1 to Regulate Thermomorphogenesis in *Arabidopsis thaliana*. *iScience* 15: 600–610.

Pubmed: [Author and Title](#)

Google Scholar: [Author Only](#) [Title Only](#) [Author and Title](#)

## Competing interests

The authors declare no competing interests.